Redox Reactions at Colloidal Semiconductor Nanocrystal Surfaces

Keaton V. Prather,‡ *Jonathan T. Stoffel*,‡ *and Emily Y. Tsui**

Department of Chemistry and Biochemistry, University of Notre Dame, Notre Dame, IN 46556, United States

ABSTRACT. The adaptation of colloidal semiconductor nanocrystals (NCs) in applications like displays, photovoltaics, and photocatalysis relies primarily on the core electronic structure of NC materials that give rise to desirable optoelectronic properties like broad absorption and size-tunable emission. However, reduction or oxidation events at localized NC surface sites can greatly affect sample stability and device efficiencies by contributing to NC degradation and carrier trapping. Understanding the local composition, structure, and electrochemical potentials of redox-active NC surface sites continues to present a challenge. In this perspective, we discuss how NC surface reduction, oxidation, and electrostatics contribute to NC electronic properties that include photoluminescence quenching or brightening and shifts in NC band edge potentials, among others. Recent efforts toward combining spectroscopic, electrochemical, and computational methods to characterize redox-active surface sites and trap states are highlighted, including developing methods in the field and future opportunities.

1. Introduction

Colloidal semiconductor nanocrystals (NCs) are nanoscale semiconductor materials capped by supporting ligands that assist in maintaining colloidal stability. Quantum confinement imparts size-tunable optical properties that enable possible applications in modern lighting, imaging, and energy storage. While NCs have been known in various forms for decades, their more recent adoption in these technologies and subsequent commercialization have been facilitated by advances in NC synthetic methods that permit improved control over NC size, monodispersity, composition, and morphology.[1-2] These improvements have also extended synthetic access to materials beyond II-VI and IV-VI lattices to III-V materials,[3-5] halide lattices,[6] and ternary compounds,[7-8] among others.

Figure 1 diagrams notable aspects of a colloidal NC. First, nanomaterials exhibit high surface-to-volume ratios. For example, a spherical zinc blende CdSe NC with a diameter of 4 nm would be calculated to have ca. 1200 atoms/NC, of which ca. 800 reside in the outermost monolayer of CdSe unit cells. This high proportion of surface atoms means that NC surfaces – that is, the semiconductor atoms that lie at the semiconductor-ligand or the semiconductor-solution interface –contribute strongly to NC physical and electronic properties.[9-11] Second, the atoms at NC surfaces display very different coordination environments compared to those within the NC core. These sites can be subject to reorganization, can display lower coordination numbers, or can be coordinated by supporting ligands or other ions.

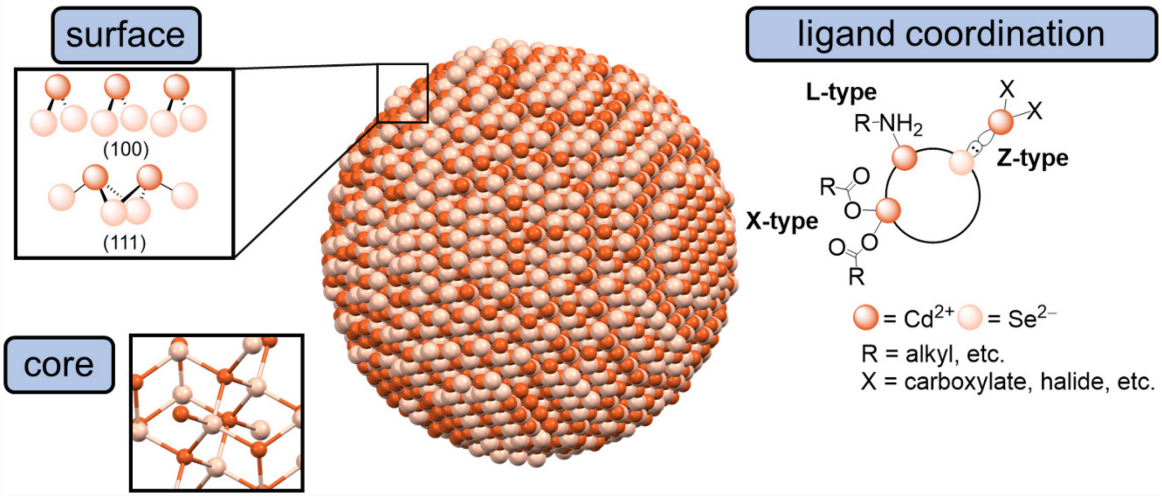

Figure 1. Schematic of a spherical zinc blende CdSe NC, showing surface and core atom geometries (left) and ligand coordination modes (right).

Figure 1 also diagrams ligand coordination at NC surfaces. Owen has popularized the categorization of these ligands by Green's covalent bond classification system, which include X-type anionic ligands, L-type neutral Lewis basic ligands, and Z-type Lewis acidic electron acceptor ligands.[12-13] This nomenclature will be used throughout this perspective. For NCs suspended in nonpolar organic solvents like hexanes or toluene, ligands are often long chain carboxylates (X-type), amines (L-type), or phosphonates (X-type), although neutral metal carboxylate or metal halide salts have been used as Z-type ligands.[14] Use of zwitterionic or charged inorganic ligands permit NC suspension in more polar solvents (e.g. formamide) or in water.[15] Ligands have also been demonstrated to contribute to the electronic structure of the NC itself through exciton delocalization or through enhancement of high energy absorption bands.[16-17] The dynamic nature of ligand-surface interactions for different NC materials has also been analyzed using NMR spectroscopy methods and by studying surface trap passivation through photoluminescence (PL) enhancement.[13-14] It is therefore important to consider NC surfaces as hybrid materials, with contributions from both surface-localized semiconductor atoms and from the coordinating ligands.

For a number of reasons, the reactivity of NC surfaces is an important consideration. First, as the surface is more exposed to solvent or other diffusing chemical species, dynamic exchange processes like ligand association and dissociation occur in solution.[18-19] This behavior may permit access to reactive surface species under room temperature conditions. Second, the different possible coordination geometries and compositions of NC surface sites result in a distribution of localized orbital energy levels, meaning that they can react as localized sites separately from the delocalized electronic band structure of the nanocrystal. Here, we will define nanocrystal surface redox as reduction or oxidation of these sites at the NC surface/ligand interface. While these processes can include ligand-centered reactions, we will primarily highlight reactions at the semiconductor atoms themselves.

In this perspective, we will discuss characteristics of NC surface redox reactions. As binary metal chalcogenide and metal oxide NCs (II-VI and IV-VI lattices) have been the most studied materials, their reactions will constitute the majority of the discussion. Additional results from recent materials like III-V materials or halide lattices will also be included when relevant. We will present optical and electrochemical evidence for surface redox processes in NC materials, both in solution and as deposited films or as part of larger assemblies. These data will be compared to those from measurements of NC surface electrostatics. The contributions of these surface-centered processes to NC stability, PL, carrier trapping, charge transfer, and band edge potentials will be included. Last, we will discuss ongoing questions and future areas of interest in NC surface redox chemistry. This perspective assumes a passing familiarity with a number of NC characterization methods. The interested reader is encouraged to access recently published reviews on these methods, which include NMR spectroscopy, X-ray photoelectron spectroscopy (XPS), and electrochemical methods.[20-23]

2. NC Surface Redox Chemistry

2.1. Irreversible surface oxidation and reduction. In semiconductor materials, surface redox has long been associated with irreversible chemical changes that are detrimental to targeted semiconductor applications in photovoltaics and photoelectrochemical cells. For example, Si and other main group semiconductor electrodes commonly form insulating oxide layers that can result in poor interfacial charge transfer.[24] In binary and higher order semiconductor materials, oxidation of surface anions initiates anodic corrosion processes. For example, oxidation of CdS photoelectrodes has been demonstrated to proceed by the decomposition pathways shown in Equations 1 and 2, releasing Cd^{2+} ions and oxidized chalcogen products.[25-27]

$$CdS + 2H_2O \xrightarrow{light} Cd^{2+}(aq) + S + H_2 + 2\ OH^- \quad (1)$$

$$CdS + 2O_2 \xrightarrow{light} Cd^{2+}(aq) + SO_4^{2-} \quad (2)$$

Metal oxide materials, although more stable than the chalcogenides, can similarly undergo photocorrosion processes under certain conditions.[28-29] In these systems, surface states have also been shown to contribute to other electronic changes within the semiconductor material, including Fermi level pinning.[30]

A number of strategies have been implemented to combat photocorrosion and other redox degradation in bulk semiconductor materials. For main group semiconductor electrodes, chemical functionalization of the semiconductor electrode surfaces has been employed to combat surface oxidation.[31-33] For CdS and CdSe electodes, redox-active electrolytes (e.g. polysulfide solutions and $[Fe(CN)_6]^{3-}/[Fe(CN)_6]^{4-}$ solutions, among others) that remove photogenerated holes from the material have been used to prevent anodic corrosion and to improve photostability.[34-35]

Nanoscale semiconductor materials employed in similar photoelectrochemical applications such as photocatalytic H_2 formation[36-39] or in quantum dot sensitized solar cells[40-41] are similarly

susceptible to anodic photocorrosion.[42-43] In II-VI, IV-VI, and III-V materials (e.g. CdS, CdSe, PbS, PbSe, InP), the main group anions (e.g. S^{2-}, Se^{2-}, P^{3-}, etc.) readily form oxide layers that have been observed by surface-sensitive elemental analysis methods like XPS and Auger electron spectroscopy (AES).[44-52] For example, exposure of CdSe NCs to air both with and without irradiation for 20-24 hours results in the formation of SeO_2, as measured by XPS.[53-54] This photocorrosion has been suggested to occur due to surface adsorption of dioxygen as well as at surface defects that facilitate reactions with air.[55] For binary semiconductor NCs, redox reactions at the metal cations are less common, although some metal oxide materials can undergo metal cation reduction to metal(0) under some circumstances. For example, Cu_2O NCs prepared under anaerobic conditions have been shown to exhibit a surface layer of Cu^0.[56] This strategy has also been used to decorate ZnO and TiO_2 nanostructures with noble metal nanoparticles (e.g. Ag, Au, Pd) for photocatalysis.[57-58]

Strategies similar to those used for bulk materials have been implemented to improve the surface stabilities of nanomaterials. For example, redox-active sulfide/polysulfide electrolytes have been used to combat surface oxidation in NC photoelectrodes.[59-60] Additional NC-specific strategies have included the addition of protective surface ligands or the growth of additional shell layers.[45, 53, 61] For example, CdSe/CdS core-shell NCs showed no surface oxidation upon irradiation under air, in comparison with unshelled CdSe NCs that underwent etching and surface oxidation.[62] Similar shelling methods have also been used to protect more sensitive NC materials like InP.[61]

2.2 "Reversible" surface reduction and oxidation. Beyond irreversible NC surface oxidation or reduction that results in NC size changes or other corrosion/deposition processes, semiconductor NCs can be considered to undergo "reversible" redox reactions. For example, carrier trapping at mid-gap energy levels implicitly reduces or oxidizes a localized orbital. Scheme 1A compares hole

trapping and electron trapping processes in a typical NC. As these mid-gap trap states in NCs are typically proposed to reside at the NC surface, these reactions must therefore be "surface redox" changes. These processes must also be reversible, as carrier de-trapping or other recombination processes have been observed spectroscopically. Additional surface redox reactions have been proposed upon chemical and electrochemical treatments of NCs. In this section, spectroscopic evidence for these redox reactions for different NC materials will be discussed.

Scheme 1. (A) Comparison of electron and hole trapping processes. (B) Surface states are reduced prior to *n*-type doping.

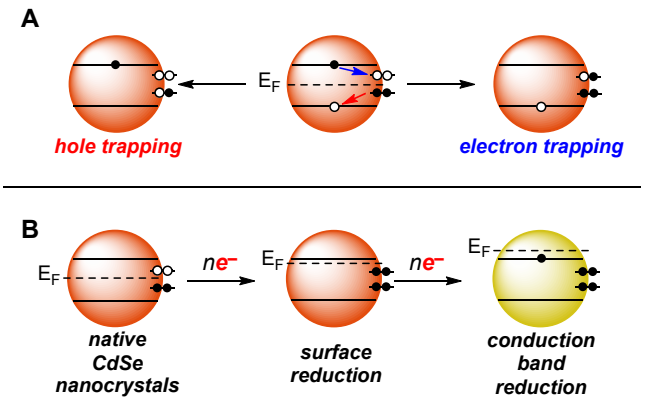

Surface redox should be distinguished from other types of redox processes like NC doping, in which the NC conduction band is occupied by electrons or the valence band is occupied by holes (*n*-type or *p*-type doping, respectively). In II-VI and IV-VI NC materials (e.g. ZnO, CdS, CdSe, PbS, etc.), spectroscopic signatures of *n*-type doping include bleaching of the excitonic absorption features, accompanied by a rise of lower energy bands corresponding to intraband transitions.[63] This *n*-type doping has been experimentally accomplished in colloidal solution by the addition of strongly reducing chemical reagents [e.g. sodium biphenyl (E^o = –3.10 V vs. the ferrocenium/ferrocene couple, Fc^+/Fc, in DMF), sodium naphthalenide (E^o = –3.10 V vs. Fc^+/Fc

in THF), or cobaltocene (E^o = –1.33 V vs. Fc^+/Fc in CH_2Cl_2)],[63-67] through photochemical electronic doping ("photodoping"),[66, 68-69] or by using electrochemically applied potentials.[70-71]

During the above reduction experiments, surface-centered reduction occurs *before* doping. A complete bleach of the lowest energy excitonic feature in CdSe or CdS NCs ($1S_{3/2(h)} \rightarrow 1S_e$) should require only two electrons in the $1S_e$ energy level. However, both chemical and photodoping methods require the addition of excess reducing agent (>10 equiv/NC) prior to the observation of a bleach in the excitonic absorption feature. Solvent and ligand reduction have been ruled out experimentally, suggesting that NC surface states are the acceptors of these "extra" electrons.[72] Similar effects have been observed in spectroelectrochemical studies, in which 10-150 electrons can be injected into colloidal CdSe NCs prior to absorption band bleaching that indicates conduction band occupation.[71] Scheme 1B diagrams this proposal. When the the Fermi level (E_F) of the solution or of the NC film is raised by the addition of reducing equivalents or by a negative applied potential, lower energy mid-gap surface states are first reduced prior to occupation of the conduction band.

Both steady-state and time-resolved emission spectroscopy can be used to indirectly observe surface redox processes. Examples discussed here will be limited to steady-state PL measurements, as the PL lifetimes of NCs (ns–μs) are often far shorter than the timescales of chemical reactions (ms–s). Although these methods do not yield structural or compositional information about traps, when used in tandem with chemical, electrochemical, and photochemical techniques, PL can be used to probe the NC surface. Gamelin and co-workers showed that addition of NaK_2, a chemical reductant, to colloidal Mn^{2+}-doped ZnSe NCs (Mn^{2+}:ZnSe) results in brightening of the manganese-centered PL ($^4T_1 \rightarrow {}^6A_1$) by up to 25-fold (Fig. 2A). This effect was rationalized as occupation of surface electron traps upon surface reduction; this occupation lowers the probability

of electron trapping and increases NC photoluminescence quantum yield (PLQY).[73] The addition of other reductants with different reduction potentials [e.g. cobaltocene and sodium anthracenide (E^o = –2.47 V vs. Fc^+/Fc in glyme)][67] resulted in different PL brightening responses, with the addition of sodium anthracenide (300 equiv/NC) achieving a maximum PLQY of 80%. These results suggest that these surface levels exhibit a range of reduction potentials. In related experiments, *electro*brightening (40-fold) of Mn^{2+}:ZnSe NCs films deposited on fluorine-doped tin oxide (FTO) electrodes was observed upon electrochemical application of negative (reducing) potentials (–1.5 V vs. Ag^+/Ag^0).[74]

The PL response to surface reduction or oxidation is material-dependent. Application of reducing potentials (<–1.5 V vs. Ag^+/Ag^0) to colloidal CdSe/ZnS or CdSe NCs results in PL quenching assigned as electron injection to the conduction band (Fig. 2B).[71, 75] This *n*-type doping results in PL quenching via a trion Auger mechanism.[76] However, when the potential is reset to 0 V vs Ag^+/Ag^0 and the NCs are no longer *n*-doped, the NC PL recovers only slowly. This slow NC PL recovery appears to correspond to slow removal of electrons from surface mid-gap states.[77] This behavior is therefore consistent with surface-charge-induced PL quenching, which has been proposed to occur by trion Auger via surface-trapped carriers.[78-79]

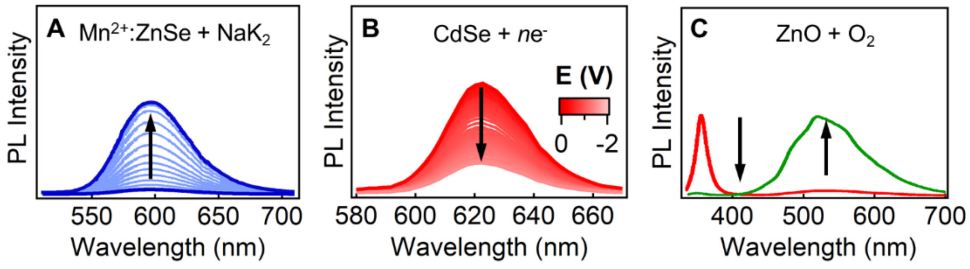

Figure 2. (A) Addition of NaK_2 increases PL of colloidal Mn^{2+}:ZnSe NCs. Adapted with permission from Rinehart, J. D., Weaver, A. L., Gamelin, D. R. *J. Am. Chem. Soc.* **2012**, *134*, 16175-16177. Copyright 2012 American Chemical Society. (B) Negative applied potentials

decrease PL of colloidal CdSe NCs prior to conduction band occupation. Adapted with permission from Ashokan, A., Mulvaney, P. *Chem. Mater.* **2021**, *33*, 1353-1362. Copyright 2021 American Chemical Society. (C) Exposure of ZnO NCs to O_2 under UV irradiation results in increased trap emission (green) compared to as-prepared ZnO NCs that primarily exhibit excitonic emission (red). Adapted with permission from Zhang, W., Chen, X., Ma, Y., Xu, Z., Wu, L., Yang, Y., Tsang, S.-W., Chen, S. Positive Aging Effect of ZnO Nanoparticles Induced by Surface Stabilization. *J. Phys. Chem. Lett.* **2020**, *11*, 5863-5870. Copyright 2020 American Chemical Society.

Surface-trapped charges can be optically active. Guyot-Sionnest and co-workers reported that the electronic absorption spectrum of CdSe NCs treated with sodium biphenyl shows a broad tail to the CdSe excitonic absorption band.[76] This feature persists after recovery of the excitonic bleach associated with *n*-type doping and is assigned to excitation of surface localized electrons to vacant higher energy levels in the conduction band. The intensity of this broad feature was used to quantify 8-10 electrons trapped on the surface. In some situations, NC samples with surface-trapped carriers can display lower energy emission bands that correspond to "trap emission," or radiative recombination from trap states. Characteristically broad trap luminescence has been observed in materials CdSe,[81] CdS,[82] and ZnO NCs.[80, 83-84] Because trap emission arises from trapped electrons and holes, surface reduction or oxidation can be used in some cases to enhance or mitigate this process. For example, oxidation of selenium at CdSe NC surfaces has been shown to enhance both band edge and trap emission; this effect was proposed to occur due to passivation of hole traps at facets that are likely to undergo nonradiative relaxation.[85] Figure 2C shows a second example, in which the addition of O_2 to ZnO NCs resulted in increased trap emission compared to band edge emission. The authors proposed that this effect occurs due to reduction of

adsorbed O_2 molecules to superoxide anions, followed by the formation of surface zinc hydroxide moieties that have been previously correlated with greater trap emission.[80, 83]

Under prolonged irradiation, photoinduced surface redox or NC charging can result in changes to NC PLQY, which can manifest as photobrightening[86-88] or photodarkening.[89-91] These effects have been primarily studied with CdSe NCs, but photobrightening or photodarkening processes have been reported for other materials like PbS,[92] InP,[93] and Si.[94] Proposed mechanisms suggest involvement of the NC surface, although the precise origin of these effects remains under debate. For example, oxidation of the surface under O_2 and passivation by water have been proposed to result in photodarkening[89] and photobrightening,[90,95] respectively. Photoinduced charge trapping has also been proposed to induce surface rearrangement or ligand desorption, causing a change in PLQY.[96] Often these PLQY changes are described as "irreversible,"[92, 97] but some photobrightened or photodarkened samples have been demonstrated to undergo slow recovery processes (hours to days).[87, 98]

Lastly, fluorescence intermittency, or "blinking," has also been associated with NC surface defects and photoionization. In CdSe NCs, blinking statistics have been shown to be sensitive to ligand passivation[99] and to surface charging.[100] Bawendi and co-workers have also shown that spectral diffusion and blinking can be affected by applied electric fields.[101-102] As with photobrightening and photodarkening, however, multiple surface-centered mechanisms have been proposed to explain the microscopic chemical origins of blinking, with little consensus.

2.3. *Structures of redox-active surface sites.* As described above, the molecular nature of the surface-localized electron acceptors or donors involved in trapping or other NC surface redox processes is not yet well understood, but is critical for rational control over NC properties. In this section, we will discuss current proposals of chemical species that may be involved in NC surface

redox reactions. Most trivially, surface ligands and adsorbates can be redox-accessible molecules that may influence surface-mediated reduction and oxidation pathways. For example, ligands like thiolates and chalcogenide anions are readily oxidized by photogenerated holes, resulting in PL quenching.[103-105] Similarly, surface-adsorbed oxygen can effect both PL quenching or brightening via competing mechanisms;[106-107] under photoexcitation, oxygen can oxidize surface chalcogenides of CdSe NCs, forming new surface defects that can trap photoexcited carriers and quench PL. However, O_2 has also been proposed to act to remove surface-trapped electrons and to eliminate competing negative trion Auger recombination in photoreduced CdSe NCs, resulting in PL enhancement.[62] These opposing observations highlight the major challenges in systematically studying NC surfaces, given the variety of samples and experimental conditions that have been published in the literature.

When considering NC surfaces from a "molecular-level" perspective,[20] there are a number of possible structural motifs that the NC surface atoms themselves can access that may be redox-active. Scheme 2 shows a selection of possible molecular structures at an example metal chalcogenide NC surface that have been proposed from computational and experimental studies, as well as how they may interconvert due to reduction or oxidation. Whereas cations and anions within the NC lattice itself are coordinatively saturated (e.g. 6-coordinate octahedral for cubic lattices like rock salt PbS, or 4-coordinate tetrahedral for wurtzite or zinc blende lattices like CdSe), the localized structures of NC surface atoms are necessarily different. These sites can have coordination spheres that are often completed by supporting ligands; for example, metal cations at NC surfaces can also be coordinated by X-type or L-type ligand donors.[13] Alternatively, surface sites can display geometries that have lower coordination numbers or that have undergone chemical rearrangement or other structural changes such as oxidative or reductive dimerization.

Scheme 2. Surface reduction and oxidation can occur at different sites of metal chalcogenide (ME) NC surfaces. (A) Reduction of the metal cation has been proposed to form metal(0) dimers and dissociate anionic ligands. (B) Oxidation of surface chalcogenide sites has been proposed to form chalcogenide dimers.

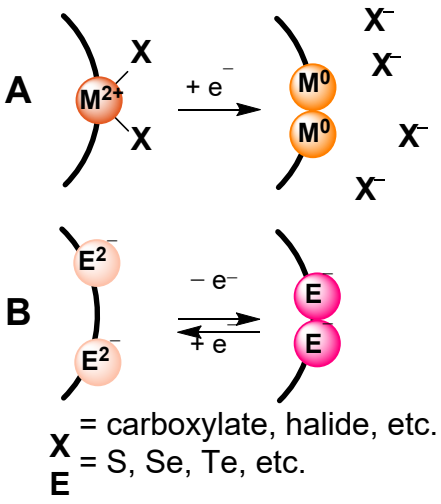

Reduction of metal ions at NC surfaces has been proposed to occur (Scheme 2A); for example, photoirradiation of CdS and CdSe NC suspensions in aqueous solutions of sulfite or other reductants was first observed to form a brown color assigned to reactive Cd^0 deposits.[108-109] Dempsey and co-workers demonstrated that treatment of oleate-capped CdSe NCs (d ~ 3.4 nm) with sodium naphthalenide as a chemical reductant formed resonances in the ^{1}H NMR spectrum corresponding to dissociated anionic oleate ligands prior to NC conduction band occupation.[64] The authors proposed that oleate anions dissociate as a charge-balancing mechanism upon localized reduction of surface Cd^{2+} ions. Pb^{2+} reduction to Pb^0 at PbS NC surfaces was similarly assigned upon treatment of the NC sample with $CoCp_2$; intriguingly, this reduction is dependent on NC size, suggesting that Pb^{2+} ions at edges may be more reducible than those at (100) facets.[65]

Metal cation reduction has not yet been directly observed experimentally, however. As of yet, XPS measurements have not been sensitive enough to observe Cd^0 or Pb^0 at CdSe or PbS NC

surfaces. DFT studies suggest that low-coordinate (e.g. two- and three-coordinate) Cd^{2+} ions only minimally contribute to surface sites that result in mid-gap levels, as these species would display linear or trigonal planar geometries, respectively.[110] Nevertheless, computational work on PbS and CdTe NCs have proposed the formation of Pb-Pb and Cd-Cd dimers upon injection of electrons.[111-112] Related DFT studies of CdSe NCs showed that photoexcitation results in electron localization at cadmium and the formation of transient metal-centered trap states.[113]

Reduction or oxidation at surface anions has also been proposed (Scheme 2B). Computational studies of CdSe NCs have assigned two-coordinate selenide ions as hole traps; these locally C_{2v}-symmetric sites would be expected to display readily oxidized selenium-centered non-bonding orbitals.[110] Figure 3 shows the MO diagram of such a site, in which the Cd and Se valence orbitals of a *localized* site, labeled with their corresponding Mulliken symbols (e.g. a_1, b_1, etc.), combine to form molecular orbitals; the HOMO of such a species would be an entirely Se-centered orbital. Hole trapping (and subsequent oxidation) of Se^{2-} (or S^{2-}) by a single electron could form a chalcogen radical – such selenium or sulfur-centered radicals have been previously detected in molecular systems as thiyl or polysulfur radicals.[114] Coupling of radicals could form Se-Se and S-S dimers that have been computationally proposed.[112] The presence of such oxidized chalcogen species has been inferred experimentally from chemical reduction of CdSe and PbS NC surfaces.[72, 64, 108] It should be noted, however, that the redox chemistry of chalcogens might also mean that higher oxidation state species are reversibly accessible, including polychalcogenides, zero-valent species (e.g. Se^0 and S^0), or oxides. As with metal-centered reduction, however, *direct* experimental confirmation of these species is limited.

For lattices containing other anions, similar anion redox may be possible. In metal oxide materials, oxygen-centered redox (for example, to form peroxides) have been invoked during

battery applications.[115] Group V anions like nitrides, phosphides, and arsenides are also sensitive and prone to oxidation, degrading to the corresponding metal oxides; in these systems, however, intermediate oxidation states have not been observed or proposed.[49, 51, 116] Last, in halide lattices, iodide oxidation to release molecular I_2 has been proposed with halide perovskite materials.[117-118]

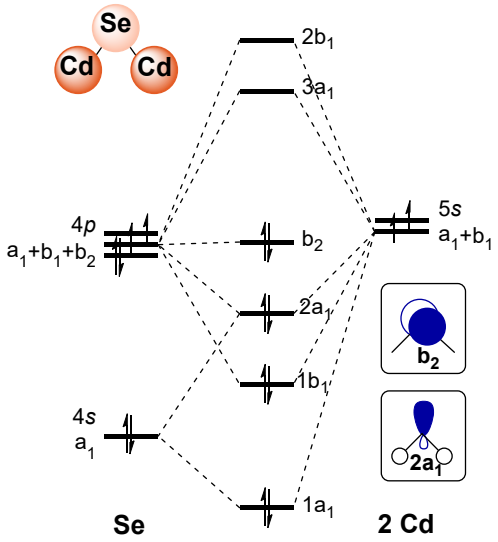

Figure 3. Diagram of relevant orbitals of two-coordinate surface selenium sites that have been proposed to act as hole traps. Mulliken symbols (a_1, b_1, etc.) correspond to the symmetries of the component atomic orbitals and of the resulting molecular orbitals.

2.4. Electrochemical potentials of surface sites. Molecular species at NC surfaces like those discussed above, whether ligand-centered or localized at the semiconductor cations or anions, undergo discrete redox events separated from the delocalized energy levels within NC bands. These redox potentials are related to chemical composition and structure and therefore may be useful for analyzing the atomistic structure of these surface states. The potentials of surface states relative to the band edges also dictates "shallow" and "deep" trap states that exhibit different carrier trapping/detrapping and thermalization processes and therefore different effects upon NC emission. For that reason, methods that can quantitatively measure the potentials of these mid-gap

orbitals and their distributions are important for distinguishing different possible trapping processes.

Electrochemical and spectroelectrochemical methods have been used to study the electronic structures of NCs (e.g. CdS, CdSe, CdTe, ZnS), and this area has been discussed in a number of recent reviews and perspectives.[21, 23, 119] These methods have largely been applied toward determining the NC band gap and the band edge potentials, and are attractive because they have been applied to NC samples both in solution[120-122] and in film.[75, 123] Figure 4A shows the cyclic voltammogram (CV) of a film of stearate-capped CdSe NCs (d ~ 7.6 nm) deposited on a glassy carbon working electrode,[124] and Figure 4B shows the CV of colloidal thioglycerol-capped CdS NCs (d ~ 3.9 nm) in DMF.[120] In these voltammograms, irreversible cathodic and anodic waves (C1 and A1, respectively) are assigned as conduction band reduction and valence band oxidation, respectively. The potential difference between these two features is called the electrochemical band gap, which can differ from the optical band gap by as much as 0.31 eV due to Coulombic effects that arise from NC charging that occurs while scanning the electrochemical potential.[125-126] This charging behavior can in some cases be avoided using differential pulse voltammetry (DPV) rather than CV.[126]

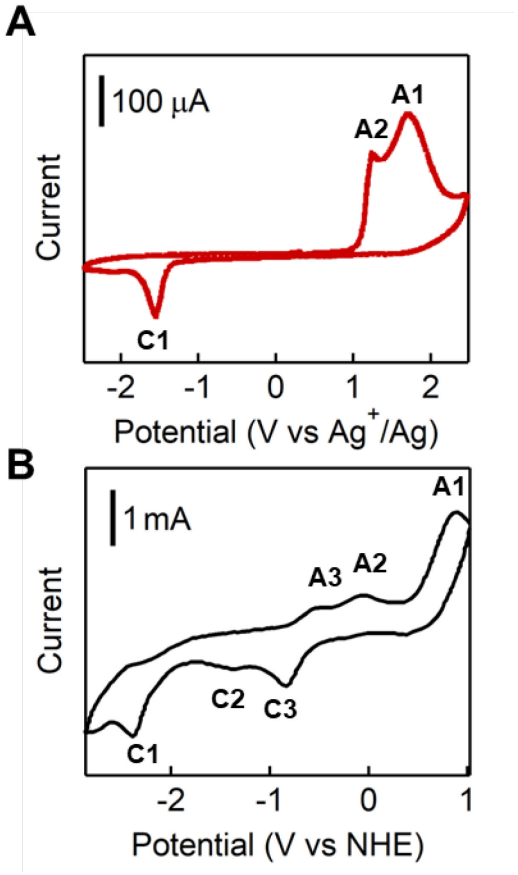

Figure 4. (A) Cyclic voltammogram of a thin film of stearate-capped CdSe NCs (d ~ 7.6 nm) drop cast on a glassy carbon electrode. The CV was measured in 0.1 M $[Bu_4N]PF_6$ in MeCN against a $AgNO_3$/Ag reference electrode. Adapted from Liu, J., Yang, W., Li, Y., Fan, L., Li, Y. *Phys. Chem. Chem. Phys.* **2014**, *16*, 4778-4788 with permission from the Royal Society of Chemistry. (B) Cyclic voltammogram of colloidal thioglycerol-capped CdS NCs (d ~ 3.9 nm) at a Pt electrode. The CV was measured in a 0.05 M THAP (THAP = tetrahexylammonium perchlorate) solution in DMF against a Ag wire quasi-reference electrode, then corrected to NHE. Adapted with permission from Haram, S. K., Quinn, B. M., Bard, A. J. *J. Am. Chem. Soc.* **2001**, *123*, 8860-8861. Copyright 2001 American Chemical Society.

Voltammograms of NC samples also display multiple additional features whose potentials lie between those of the band edges. For example, in Fig. 4A, the feature marked A2 at 1.23 V vs.

Ag^+/Ag is an anodic wave that has been assigned as irreversible surface Se^{2-} oxidation. Similar oxidation features have been observed in other materials, including CdS (Fig. 4B, A2 and A3: –0.05 and –0.54 V NHE, respectively),[120] PbS,[121] and CdTe.[127] The potentials and peak widths of these features are highly variable, however, and can shift significantly depending on NC size,[124-125, 128] capping ligands,[124, 129] as well as the solvent or electrolyte used.[124] The number of mid-gap redox features is also sample- and experiment-dependent. This variability has been proposed in some cases to arise from different facet-dependent electrochemical potentials as well as from a distribution of multiple surface oxidation states.[125, 130] Despite the common assignment of mid-gap redox waves in NC voltammograms as reduction and oxidation of surface sites on the NCs,[120, 130] it should be noted that voltammetry only measures electron transfer processes and cannot distinguish between charge transfer to surface states, ligands, or other NC electronic states.

Typically, voltammograms of II-VI and IV-VI materials show large, electrochemically irreversible, anodic waves, and any cathodic processes assigned as surface reduction exhibit much smaller currents. The irreversibility of these features suggests that fast electron transfer can be coupled to slower chemical reactions, that is, an EC process, or other related mechanisms.[131] These coupled mechanisms may therefore indicate that the *reversible* picosecond dynamics that have been spectroscopically observed do not show the full chemical picture of surface redox. Along similar lines, Cossairt and co-workers have demonstrated that photoinduced charge transfer from NCs to molecular charge acceptors occur at rates on the order of 0.1 s^{-1}, many orders of magnitude slower than those of ultrafast spectroscopic dynamics that have been previously reported.[132]

Other electrochemical methods that were previously applied toward the analysis of bulk semiconductor materials have been recently turned toward the analysis of NC films. For example, surface photovoltage spectroscopy (SPV)[133-135] has been used to measure both the carrier type and

potentials of surface traps in relation to band edge potentials. In one study, Brutchey and Osterloh demonstrated that halide-terminated CdSe(CdX_2) NC films (X = Cl^-, Br^-, I^-) displayed halide-dependent hole trap potentials (140–210 meV), and that the coordination or removal of butylamine changed the distribution and density of electron trap states.[129] Electrochemical impedance spectroscopy (EIS)[136,137] has been similarly used to analyze the potentials and density of states of NC films. While these studies have been primarily used to compare to data acquired using voltammetry and to study the band edge potentials, studies of PbS NC films were able to identify a trap state manifold 190 meV below the conduction band edge and to measure its density of states.[138] Further measurements were used to assign the mechanism of PbS charging and electron trapping as a PbS NC dimerization model rather than other surface site rearrangements.[139] In the long term, these methods will likely provide deeper insight into NC surface chemistry compared to standard voltammetric techniques.

Table 1 lists variations in these mid-gap redox potentials of selected NC samples, calculated here as the difference between the potential of the mid-gap anodic feature ($E_{s,a}$) and the anodic wave assigned as valence band oxidation (E_{VB}). Additional parameters, including the NC size, capping ligand, electrochemical method used, and both the optical and electrochemical band gaps (ΔE_g^{opt} and ΔE_g^{ele}, respectively) are included. The absence of a clear trend in these data or these features demonstrate the high sample-to-sample variability in surface state potentials measured using this method, supporting a need in the field toward NC surface standardization.

Table 1. Comparison of the electrochemically measured trap depth, $E_{VB} - E_{s,a}$, for different NC samples.

Material	***d*** **(nm)**	**Capping Ligand**[c]	**Method**	$E_{VB} - E_{s,a}$ **(meV)**	ΔE_g^{opt} **(eV)**	ΔE_g^{ele} **(eV)**	**Ref**

CdSe	3.23	TOPO[d]	CV	700	2.17	2.10	[128]
	3.48	TOPO	CV	900	2.13	2.03	
	3.73	TOPO	CV	950	2.08	1.99	
	[a]	ODPA + Cl	CV	700			[130]
	[a]	ODPA + Cl	CV	300			
	[b]	ODPA	CV	300			
	4.54	$CdCl_2$	SPV	450	2.08[e]	2.07	[129]
	4.54	$CdBr_2$	SPV	250	2.08[e]	2.05	
CdTe	2.8	TGA	CV	520	2.26	1.95	[125]
	3.3	TGA	CV	465	2.13	1.91	
	3.6	TGA	CV	380	1.96	1.85	
ZnSe	2.1	TGA	CV	555			[140]
	1.9	TGA	CV	400			
PbS	3.24	Methanethiol	EIS	190	1.14	1.0	[138]

[a]Pyramidal-shaped NCs. [b]Rod-shaped NCs. [c]ODPA = octyldecylphosphonic acid, TGA = thioglycolic acid, TOPO = trioctylphosphine oxide. [d]It has been noted that "TOPO"-capped NCs are likely supported by phosphonate and other phosphinic acid impurities in the commercial TOPO reagent.[141] [e]Estimated from reported NC size.

2.5. Toward better characterization of surface redox. Spectroscopic techniques for NC surface characterization continue to advance, and we expect that a number of methods will soon enable deeper understanding of the molecular structures and dynamics of localized surface sites.

NMR spectroscopy. Solution NMR spectroscopy has long been used to study ligand coordination to colloidal NCs.[142] In particular, ^{1}H NMR spectroscopy distinguishes ligands that are bound to NC surfaces from those free in solution.[13, 64] 2D NMR methods provide additional information. For example, nuclear Overhauser effect spectroscopy (NOESY) gives information on ligand-NC interactions through space,[19] while diffusion ordered spectroscopy (DOSY) can be used

to quantify ligand binding by the calculation of diffusion constants.[143-144] These methods have also been applied toward studying NC ligand exchange reactions,[145] and can also indicate the relative purity of NC samples.[146] Heteronuclear NMR spectroscopy can be applied to study certain NC ligands; for example, ^{31}P NMR spectroscopy has been used to study the coordination of phosphorus-containing ligands such as phosphines or substituted phosphonic acids.[147] ^{113}Cd NMR spectroscopy has also been used to characterize cadmium carboxylate complexes that can in principle act as Z-type ligands.[148] This method has not yet been applied to studying surface ligand binding, but has been used to study the mechanism of NC formation.[149]

Beyond ^{1}H NMR spectroscopy of NC ligands, there have been efforts to use heteronuclear NMR spectroscopy of spin-active nuclei comprising the NC lattices themselves. These experiments are often conducted using solid-state NMR (ssNMR) techniques, particularly when coupled with magic angle spinning (MAS).[150] For example, ^{31}P NMR spectroscopy has been used to characterize InP NCs to identify oxidized phosphorus sites.[151-152] MAS experiments and 2D NMR methods have also been used with ^{113}Cd and ^{77}Se nuclei to characterize CdSe NCs.[153-154] While these did not explicitly address surface redox, multiple ^{77}Se resonances were observed, some of which were assigned as different surface sites. Despite the utility of ssNMR MAS, there are a number of drawbacks. Even with the resolution enhancement offered by MAS, the method itself has low sensitivity and requires hundreds to thousands of scans and many hours.[153, 155-158]

In recent years, dynamic nuclear polarization (DNP) enhanced MAS NMR spectroscopy has been used to overcome the sensitivity issues of MAS NMR methods.[159-160] Transfer of spin polarization from added stable organic radicals to the nuclear spin enhances the measurement up to 100-fold, resulting in shorter measurement times by 2-4 orders of magnitude and experiment times of tens of minutes.[161-162] Importantly, DNP enhanced NMR increases the intensity of

resonances corresponding to nuclei at the NC surface. Studies by Kovalenko, Rossini, and others of CdSe NCs have been able to reveal the coordination environment of core and surface Cd^{2+} and Se^{2-} centers.[161, 163-164] These methods have also been applied toward other materials such as lead halide perovskite films[165] and alkaline earth chalcogenide NCs.[166]

DNP surface enhanced MAS NMR methods will likely soon provide opportunities to characterize NC surface redox chemistry. While these methods are not fast enough to be used yet for in situ measurement of chemical reactions, (i.e. seconds or faster), it would still be possible to induce surface changes via chemical, photochemical, or electrochemical treatment prior to NMR measurement.

EPR spectroscopy. Electron paramagnetic resonance (EPR) spectroscopy has long been applied to semiconductor materials, beginning with measuring defects in silicon.[167] In binary materials, microcrystalline and nanocrystalline ZnO has been observed to display EPR signals assigned as oxygen vacancies.[168-170] In TiO_2, paramagnetic Ti^{3+} formed from electron trapping at Ti^{4+} was also observed at 4.2 K.[171] EPR spectroscopy of metal chalcogenide semiconductor materials is less common, although CdSe NCs have been shown to form hydroxyl radicals in aqueous solution under irradiation.[172]

Along with studying defects such as vacancies, EPR spectroscopy has also been used to detect transition metal ion dopants (e.g. Mn^{2+}, Co^{2+}) in semiconductor materials, also called dilute magnetic semiconductor (DMS) materials,[173-174] as well as surface impurities.[175] Gamelin and co-workers showed that for Mn^{2+}-doped ZnO NCs (Mn^{2+}:ZnO), the EPR signals of surface-bound Mn^{2+} ions are broadened in comparison to Mn^{2+} in the ZnO lattice due to inhomogeneity in environments at the surface.[173] Similar spectra were observed for Mn^{2+}:CdSe NC samples.[176] While EPR spectroscopy of these doped DMS NC materials would not necessarily provide

information regarding surface redox, it may in the future be possible to use these paramagnetic centers at NC surfaces to report on the different electronic environments at the NC surface.

There have also been a number of elegant experiments using EPR spectroscopy of NC ligands that display unpaired electrons. Separately, Scaiano and Beaulac have studied CdSe NCs modified with radical ligands (4-carboxyphenylnitronyl nitroxide and 4-amino-TEMPO radicals).[177-179] These show an interaction between the unpaired electron of the ligand and the NC which results in fast PL quenching. For these systems, EPR spectroscopy was primarily used to confirm that the radical-containing ligands were unmodified prior to photoexcitation. Scaiano and co-workers also showed that EPR spectroscopy can be used to monitor the kinetics of disulfide addition to CdSe NC surfaces.[180] Prior to disulfide S–S bond cleavage, the radical-modified substituents exhibit a coupled diradical EPR spectrum. When coordinated to the NC surface, they exhibit free $S = ½$ signals. Last, Gamelin and co-workers have shown that irradiation of CdSe NCs in the presence of a spin trap (*N*-*tert*-butyl-α-phenylnitrone) forms a nitroxyl radical associated with the NC surface.[181]

Transmission electron microscopy (TEM). TEM has long been a tool for studying the sizes and morphologies of NCs,[182] and high-resolution TEM can distinguish different facets and atomically resolve the surfaces of the NCs.[183-184] TEM has been most commonly conducted under high vacuum conditions that are not well suited for studying surface redox processes, particularly of colloidal systems. Better surface-centered characterization may soon be possible, however, due to development of liquid phase TEM measurements, also called liquid cell electron microscopy, in which samples can remain suspended in solution phase through the use of low-vapor-pressure solvents like ionic liquids or using special TEM holders or other setups.[185] This method has already been applied toward imaging NC diffusion and growth.[186-187] More recently, liquid cell electron

microscopy has been interfaced with electrochemical perturbations or with redox control of the electrochemical potentials within the cell;[188-189] these techniques have been applied toward understanding nanocrystal etching or other degradation processes in metal nanocrystals and toward operando measurements of catalysts.[189-190] As these techniques continue to advance and resolution increases, we expect that this technique will be extremely powerful when used in tandem with other methods.

3. NC Surface Electrostatics

3.1. Factors contributing to surface electrostatics. Because surface redox events change the overall NC charge and therefore the surrounding electric field, NC surface electrostatics are intimately linked with these processes. Because colloidal semiconductor NCs are hybrid materials, the electrostatics and charge at the NC surface-solution interface is governed by multiple factors. Figure 5 diagrams some of these components, which include contributions from the surface cations and anions, the supporting ligands, and the solution media itself. We note that the complexity of the NC surface-solution interface presents challenges toward quantitative analysis of surface electrostatics, and much of the literature reports qualitative trends.

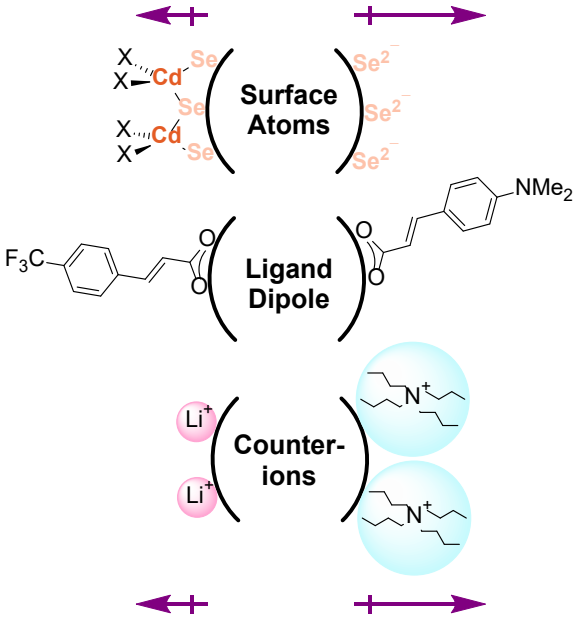

Figure 5. The surface dipole moment/electrostatic field can be tuned through post-synthetic modification of surface stoichiometry, ligands, and screening ions, among many other factors. The arrows indicate the total NC surface dipole moment.

First, for different crystal structures, particularly in anisotropic structures like nanorods, nanoplatelets, tetrapods, and others, greater exposure of different facets can contribute to a net surface dipole moment, as some facets (e.g. the (111) facet in zincblende structures) are non-centrosymmetric. This facet dependence has been applied toward understanding ligand coordination and promoting NC reactivity.[191-192]

Second, NC surface electrostatics would also be affected by the ratios between charged components and their spatial separation. For II-VI or IV-VI NCs, these would include the metal cations, chalcogenide anions, and any charged supporting ligands such as carboxylates or phosphonates. From previous studies, II-VI, IV-VI, and III-V NCs are known to be cation-rich rather than completely stoichiometric;[13] this additional positive charge is balanced by the coordination of negatively-charged X-type ligands. Additional charge compensation can occur by a number of different mechanisms, including by the formation of vacancies,[193] or by the intercalation or surface adsorption of ions (e.g. H^+, Li^+, etc.).[194-197] Surface charge can therefore be changed by altering the density of these charged ligands. An alternative way of framing NC non-stoichiometry has been in considering the stoichiometric NC in which the surface anions are coordinated by electron-accepting Z-type neutral MX_2 species (for example, cadmium carboxylate compounds).[13] Variation in Z-type ligand density could also be expected to change the surface dipole moment through interactions with polar facets, as discussed above.

One major challenge in the area of NC synthesis has long been variation between synthetic batches of NC size and dispersity; this variability also can extend to NC surface stoichiometry and

ligand coverage, which can also vary depending on the NC purification method or even upon sample dilution.[198-199] The NC surface should be considered to be dynamic, with multiple species exchanging at equilibrium. This behavior is particularly important for more ionic lattices like cesium lead halide perovskites, in which it has been shown that charged ligands exchange with ion pairs in solution, among other processes.[18] Ultimately, improved understanding over these processes is needed for greater synthetic control over NC surface electrostatics.

Third, ligands with similar charge can be tuned to affect the surface electrostatic field. Equation 3 expresses the net dipole moment normal to the NC surface (p_z) induced by surface ligands.

$$p_z = p_{\text{ligand,z}} + p_{\text{ind,z}} \quad (3)$$

This dipole moment is a sum of contributions from an intrinsic ligand dipole moment ($p_{\text{ligand,z}}$) and an induced dipole moment from coordination of the ligand donor groups to the NC surface ($p_{\text{ind,z}}$). To vary the intrinsic ligand dipole moment, Sellinger and others have synthesized series of substituted cinnamate and substituted styrylphosphonic acids in which the arene substituents vary from electron-withdrawing trifluoromethyl groups to electron-donating methoxy or amino substituents.[200-201] Typical nonpolar ligands with hydrophobic tails can also be exchanged for zwitterionic or inorganic ligands that greatly tune the surface charge and permit dispersion in polar solvents. Talapin and co-workers have shown that the surface electrostatic potentials of NCs can be tuned through ligand exchange with main group anions like S^{2-} or with thiometallate anions.[15, 202] Different short-chain ligands with polar functional groups (e.g. cysteamine, mercaptopropionic acid, etc.) permit NC suspension in water.[203] As such, the dielectric of the supporting ligands and of the solvent are also key considerations for modification of the electrostatic field near the surface.

3.2. Effects of surface electrostatics. Surface electrostatics contribute to the colloidal stability of charged nanoparticles. In stable colloidal suspensions of charged particles, repulsive double layer

effects overcome attractive van der Waals forces that promote particle aggregation. DLVO (Derjaguin, Landau, Verwey, and Overbeek) theory has been used to relate the interparticle electrostatic force to the surface charge density, the solvent dielectric, and the solution ionic strength, in which the latter two properties describe the Debye length and solution charge screening.[204] Figure 6 shows a diagram of the double layer of a charged particle that results in electrostatic repulsion for colloidal stability.

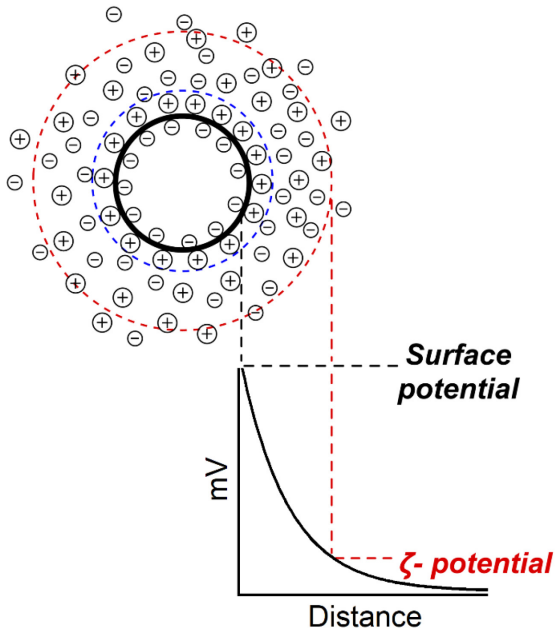

Figure 6. Charge layers around a negatively-charged colloidal NC.

Charged nanoparticle suspensions are often characterized using zeta potential (ζ-potential) analysis, which measures the electrochemical solution potential as a function of the NC electrical double layer.[205-206] For semiconductor NCs, ζ-potentials have been measured in the context of understanding NC colloidal stability in water for drug delivery and imaging applications. Ligand-exchanged CdSe NCs have been shown to be colloidally stable when |ζ-potential| > 30 mV.[203] However, both DLVO theory and ζ-potential analysis are most reliable in aqueous solutions or in polar organic solvents with high dielectric constants; in more nonpolar organic solvents, other

forces such as solute-solvent interactions have a larger effect.[207] Additionally, NCs suspended in nonpolar organic solvents are often terminated by long chain ligands; for these samples, steric repulsion by these large organic ligands may have greater contribution than electrostatic repulsion toward preventing NC aggregation. Nevertheless, if the NC surface charge is post-synthetically modified via surface reduction/oxidation or ligand exchange, it is likely that these electrostatic changes may have a non-negligible effect upon colloidal stability.

Changes to NC surface electrostatics also affect their optical features. For example, surface reduction of CdSe NCs results in red-shifting and broadening of the excitonic absorption features.[65, 208] This change has been assigned to Coulombic (electrostatic) interactions between surface-localized electrons and excitons, resulting in an apparent shift of the band edge energies.[208] This electrostatic-induced change to the observed optical band gap can also be observed during NC voltammetry experiments.[126] Electrostatics also has a strong effect on NC emission, as electric fields have been shown to quench PL by a quantum-confined Stark effect (QCSE).[101] This effect extends to surface charges. In CdSe or CdSe/ZnS NCs, PL emission has been demonstrated to be highly correlated to the zeta potential of the resulting NC sample.[209-210] In one example, ligand functional groups at the NC surface were varied, and lower absolute ζ-potentials were observed to correspond to longer average radiative lifetimes and higher PLQY.[209] While the absolute mechanism of this behavior is still not completely clear, this dependence was attributed to greater trion formation with more charged NCs, resulting in Auger recombination and PL quenching.

Due to this relationship between surface charge and PL, post-synthetic modification of NC surface charge or electrostatics has been used to control PLQY. For example, the introduction of different redox-inactive metal ions (e.g. Na^{+}, Al^{3+}, In^{3+}, Ca^{2+}, etc.) to sulfide-capped CdSe NCs resulted in control over both NC ζ-potentials and PL efficiency.[210] Similarly, Mulvaney and co-

workers demonstrated that changing the surface stoichiometry of CdSe NCs from Cd-rich to Se-rich resulted in PL quenching, although addition of phosphines reversed this process.[95] This effect of surface stoichiometry has also been extended to other materials, including CdS and Ag_2S NCs.[211-212] In the above studies, PLQY changes were attributed to trap formation, but these effects cannot be readily deconvoluted from other electrostatic contributions.

Lastly, the surface dipole moments at NC surfaces have been correlated to shifts in the band edge potentials. Figure 7 diagrams how surface dipole moments are expected to shift the absolute energies of the valence and conduction bands without changing the band gap. CV experiments and ultraviolet photoelectron spectroscopy (UPS) or XPS methods have been used to measure the valence band maxima for NC samples (InAs, CdSe, PbS, etc.) after ligand exchange both in solution and in film.[200, 213-216] Although the optical band gaps for these samples remained the same, the band edges of PbS NC films were observed to shift by over 1 eV upon ligand exchange, indicating high sensitivity to ligand effects. From calculations, these large shifts of band edge energies has been assigned to an electrostatic effect due to a surface dipole associated with the ligands.[217] Beard and co-workers have shown that substituted cinnamate ligands with dipole moments spanning from –2 to +6 Debye on PbS NCs (d ~ 3.2 nm) can result in a shift in band edge potentials of over 2.0 eV.[200] In a similar approach, Gamelin and co-workers used a potentiometric approach to measure shifts in colloidal CdSe NC conduction band edge potentials upon n-type doping.[218] For these samples, variation of the surface stoichiometry (from Cd^{2+}-enriched to Se^{2-}-enriched) was shown to shift the band edge potentials by over 400 meV.[219]

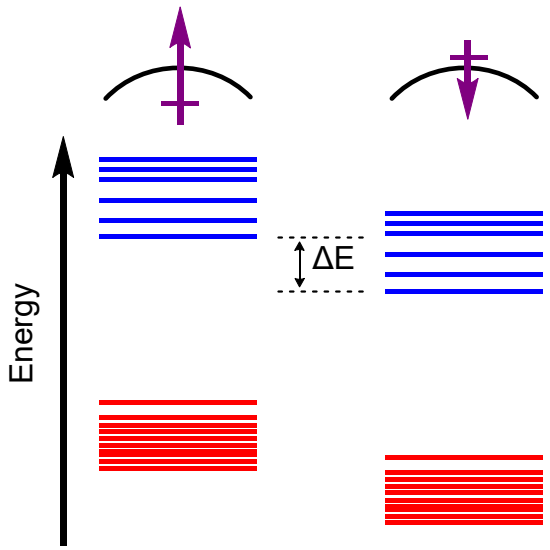

Figure 7. Changes to the total surface dipole of NCs result in shifts in the absolute energy positions of the valence band and conduction band. Diagram is not to scale.

The various methods of perturbing NC surface electrostatics therefore provide a powerful method of controlling NC band edge potentials. These shifts can be mathematically predicted using the Helmholtz equation (Eq. 4):

$$\Delta V_z = \frac{p_z}{A\varepsilon\varepsilon_0} \qquad (4)$$

where ΔV_z is the shift in the valence band potential induced by the NC surface dipole moment, p_z is the surface dipole moment encompassing the ligand contributions, A is the surface area of the ligand, and ε is the dielectric constant of the ligand layer. Thus far, this post-synthetic modification approach have been used to target redox-shifted layers for the fabrication of solar cell devices exhibiting greater efficiency and lower rates of charge recombination,[215] but has implications for many other NC applications (vide infra). Many aspects regarding standardized conditions for controlling these band edge potential shifts (e.g. solvent, additives, ligand dielectric, etc.) remain underexplored, however.

3.3. Spectroscopic reporters for surface characterization. Although the surface charge of NC films are readily measured using well-established solid-state electrochemical methods,[220] the multiple factors that can contribute to colloidal semiconductor NC surface electrostatics and the inorganic-organic hybrid nature of many sample-solution interfaces make *solution-phase* surface electrostatic/charge measurement more challenging. For example, as discussed above, ζ-potential analysis is most reliable in aqueous solution or in polar solvents (e.g. formamide) with low ionic strength, complicating analysis of NC samples that are coordinated by hydrophobic ligands and suspended in nonpolar hydrocarbon solvents.

Vibrational spectroscopic reporters have recently been used as an alternate method of characterizing colloidal NC surface electrostatics of samples suspended in nonpolar organic solvents.[221-223] This approach is conceptually related to the analysis of heterogeneous materials or films, in which molecules like carbon monoxide (CO) have long been used as probes to study catalytically active surface sites (e.g. at Pt(111)).[224-225] The frequencies and intensities of the CO bond stretches enable characterization of the catalyst surfaces using vibrational spectroscopy.[226] As CO does not readily absorb at colloidal semiconductor NC surfaces, reduced metal carbonyl species ($[Fe(CO)_4]^{2-}$, $[Co(CO)_4]^-$) were post-synthetically attached to NC surfaces (CdSe, CdS, PbS, ZnS) through X-type and Z-type ligand exchange reactions (Fig. 8A). The solution-phase IR spectra were used to assign coordination of these metal carbonyl fragments to trigonal bipyramidal geometries (Fig. 8B).

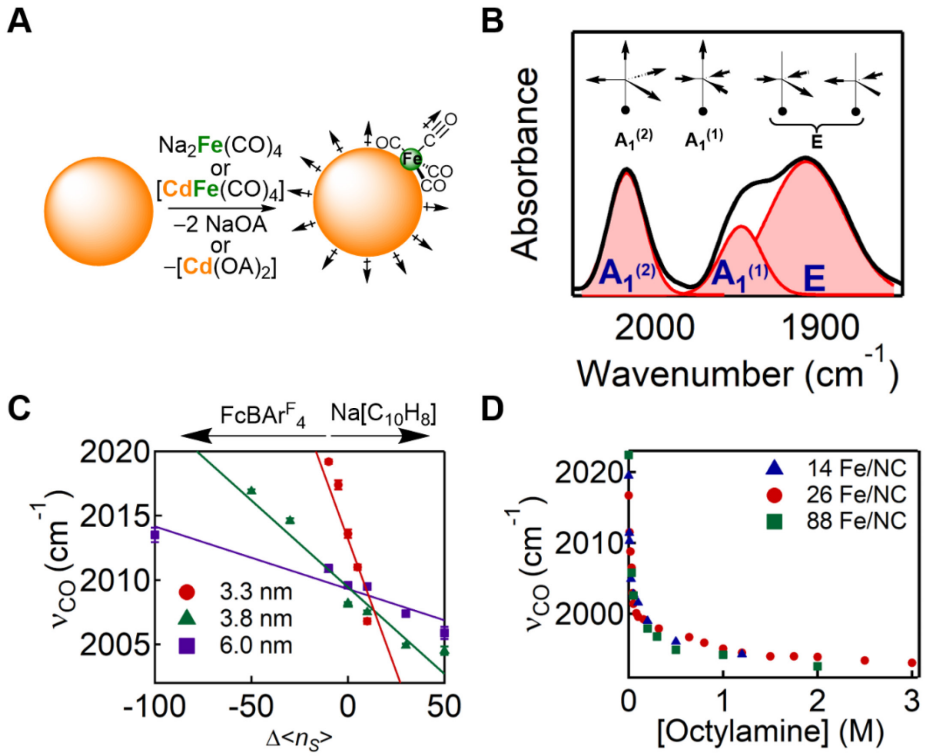

Figure 8. (A) Synthesis of metal carbonyl-functionalized NCs, and a diagram of the CO vibrational response to the NC surface dipole moment. (B) Solution-phase IR spectrum of CdSe-$CdFe(CO)_4$ NCs with assigned normal modes. The energies of the $A_1^{(2)}$ ν_{CO} bands of CdSe-$CdFe(CO)_4$ NCs respond to (C) chemical surface reduction or oxidation or to (D) changes in surface stoichiometry upon addition of octylamine. (C) was adapted with permission from Schival, K. A., Gipson, R. R., Prather, K. V., Tsui, E. Y. *Nano Lett.* **2019**, *19*, 7770-7774. Copyright 2019 American Chemical Society. (D) was reprinted with permission from Prather, K. V., Stoffel, J. T., Tsui, E. Y. *Chem. Mater.* **2022**, *34*, 3976-3984. Copyright 2022 American Chemical Society.

The energies of IR vibrations have been demonstrated to be responsive to the nearby electric Field; this phenomenon has been termed the vibrational Stark effect.[227] Electrostatic effects have also been demonstrated to affect metal carbonyl C–O stretching frequencies (ν_{CO}) energies, in addition to other electronic contributions such as π-backbonding or σ-donation.[228] As the analysis

of the ν_{CO} of molecular metal carbonyl complexes is well precedented, the normal modes of $[Fe(CO)_4]^{2-}$functionalized CdSe NCs (CdSe-$CdFe(CO)_4$ NCs) could be assigned (Fig. 8B) and normal coordinate analysis permits some quantification of the electronic effects of NC surface coordination upon the metal carbonyl center.[222] In these IR spectra, the highest energy ν_{CO} band is assigned to the all-symmetric $A_1^{(2)}$ band, in which the axial CO ligand is normal to the NC surface and therefore parallel to the NC surface dipole moment. As such, the energy of the $A_1^{(2)}$ ν_{CO} band is expected to be sensitive to the NC surface electrostatic field. However, we note that these effects are currently not deconvoluted from other NC surface properties, including ligand density and solvent dielectric, etc.

Figure 8C shows the energies of the $A_1^{(2)}$ ν_{CO} band in CdSe-$CdFe(CO)_4$ NC samples upon treatment with the chemical reductant $Na[C_{10}H_8]$ or with the oxidant ferrocenium tetrakis(3,5-bis(trifluoromethyl)phenyl)borate ($FcBAr^F_4$).[221] Surface reduction shifts the ν_{CO} band to lower energies, which is reversed upon surface oxidation. These effects are well-behaved and size-dependent, therefore enabling a qualitative measurement that can be used to standardize surface electrostatic contributions to NCs. As a demonstration of an alternative method for post-synthetic modification of NC surface electrostatics, similar shifts of the ν_{CO} band of CdSe-$CdFe(CO)_4$ NCs can be achieved upon changing the surface Cd^{2+}:Se^{2-} stoichiometry by octylamine-mediated removal of cadmium oleate ($Cd(OA)_2$) Z-type ligands (Fig. 8D).[223] Interestingly, the response of the ν_{CO} band varied upon dissociation of $Cd(OA)_2$ from two different types of surface sites, tentatively assigned as exposure of (111) and (100) facets that exhibit different surface dipole moments.[229] Altogether, these results demonstrate that the use of alternate approaches based in molecular inorganic chemistry can provide new spectroscopic methods for interrogation of complex NC surfaces.

3.4. Outlook: applications in photocatalysis. The tunable surface electrostatic dipoles of NC materials clearly underpin many NC properties. While the relation between the NC surface dipole moment and band edge potentials has been primarily used to control band edge alignment in deposited films as components of photovoltaic devices,[215] we predict that this dependence could be harnessed for additional solution-phase applications such as photocatalysis. The use of colloidal semiconductor NCs as photocatalysts is a longstanding goal in the field, beginning with early efforts in photoelectrochemical energy storage and in water splitting, as discussed earlier in this perspective. This area has advanced significantly over the past decade, including efforts in studying interfacial photoinduced charge transfer rates and the role of ligand shell permeability in several different NC systems.[230] Colloidal NCs have also been used in more modern organic photoredox reactions.[231-234] Opportunities and challenges in this area have been discussed in recently published perspective articles.[235-237]

Surface electrostatics are *already* known to impact photocatalysis by impacting chemisorption of substrates. Weiss and co-workers have demonstrated that CdS NCs with chalcogenide-enriched surfaces exhibit faster charge-transfer to methyl viologen. This effect was attributed to greater adsorption of the substrate to the NC surface.[238] An opportunity here is that while it is challenging to modify the surface metal:chalcogenide ratio in situ, it may be possible to tune catalytic rates mid-reaction through surface reduction or oxidation. This process may therefore enable switchable photocatalysis reactions.

The response of band edge potentials to the surface dipole moment likely plays a significant role in NC photocatalysis. Given that band edge potentials can shift by more than 1 eV, such surface modifications would greatly impact driving forces for the reactions, as the potentials of excited states of photocatalysts are critical.[239] This may offer opportunities in targeting heavily studied,

but currently challenging aspects of small molecule activation such as CO_2 reduction or N_2 reduction. In essence, tuning the potentials to more negative reduction potentials could facilitate electron transfer to these difficult-to-reduce molecules. Post-synthetic surface modification and NC electrostatic tuning may also prevent photocorrosion by shifting the band edges such that anodic photocorrosion potentials do not lie within the band gap, therefore favoring intermolecular charge transfer over surface degradation. Alternatively, there may be synthetic opportunities to tune surface redox itself to favor reversible redox processes over irreversible surface photodegradation like the formation of oxides.

4. Summary and Outlook

Although the field of colloidal semiconductor NCs is comparatively mature from optical spectroscopy and synthetic perspectives, it is clear that understanding the chemical and electrochemical reactions at NC surfaces remains an outstanding challenge. Questions still remain for 1) identifying the compositions and structures that form redox-active surface sites and traps in different NC materials, 2) understanding what factors govern their electrochemical potentials, and 3) deconvoluting the effects of different types of surface sites and surface electrostatics upon NC PL and charge transfer.

While our understanding of NC surfaces has grown, achieving a comprehensive picture of dynamic interplay between NC surface atoms, ligands, and charges, particularly for colloidal samples, will likely require nanocrystal-specific techniques beyond standard materials characterization methods. Developing new approaches that combine spectroscopic, electrochemical, and computational methods and that can probe NC processes on the longer timescales of chemical reactions is therefore a priority. One major challenge in this regard is finding ways to study NC samples without perturbing the surfaces themselves, as NC surfaces are

sensitive to solvent, concentration, size, ligand coverage, and solution resting potential, and can vary greatly from sample to sample.

AUTHOR INFORMATION

Corresponding Author

*E-mail: etsui@nd.edu

Author Contributions

The manuscript was written through contributions of all authors. All authors have given approval to the final version of the manuscript. ‡These authors contributed equally.

Biographies

Keaton Prather earned his B.S. degree from the University of Kansas and his Ph.D. in chemistry from the University of Notre Dame. His research focuses on probing nanocrystal surface electrostatics using spectroscopic reporters. He has been awarded the University of Notre Dame Department of Chemistry and Biochemistry Dow Outstanding Graduate Student Award.

Jonathan Stoffel earned his B.S. degree from California State Polytechnic University, Pomona and is currently a Ph.D. candidate at the University of Notre Dame. His research focuses on spectroscopic and electrochemical characterization of nanocrystal surfaces. He is the recipient of numerous awards.

Emily Tsui received her Ph.D. in chemistry from the California Institute of Technology and completed her postdoctoral studies at the University of Washington. She is an assistant professor of chemistry at the University of Notre Dame, where she studies sulfur chemistry at transition metal sites relevant to biology and the surfaces of semiconductor nanocrystals.

ACKNOWLEDGMENT

This work was supported by the University of Notre Dame and by the NSF (CHE-2154948).

K.P. is supported by an Arthur Schmitt fellowship and a ND CEST fellowship.

REFERENCES

1. Murray, C. B., Norris, D. J., Bawendi, M. G. Synthesis and Characterization of Nearly Monodisperse CdE (E = Sulfur, Selenium, Tellurium) Semiconductor Nanocrystallites. *J. Am. Chem. Soc.* **1993**, *115*, 8706-8715.
2. Hendricks, M. P., Campos, M. P., Cleveland, G. T., Jen-La Plante, I., Owen, J. S. A Tunable Library of Substituted Thiourea Precursors to Metal Sulfide Nanocrystals. *Science* **2015**, *348*, 1226-1230.
3. Battaglia, D., Peng, X. Formation of High Quality InP and InAs Nanocrystals in a Noncoordinating Solvent. *Nano Lett.* **2002**, *2*, 1027-1030.
4. Allen, P. M., Walker, B. J., Bawendi, M. G. Mechanistic Insights into the Formation of InP Quantum Dots. *Angew. Chem. Int. Ed.* **2010**, *49*, 760-762.
5. Gary, D. C., Glassy, B. A., Cossairt, B. M. Investigation of Indium Phosphide Quantum Dot Nucleation and Growth Utilizing Triarylsilylphosphine Precursors. *Chem. Mater.* **2014**, *26*, 1734-1744.
6. Protesescu, L., Yakunin, S., Bodnarchuk, M. I., Krieg, F., Caputo, R., Hendon, C. H., Yang, R. X., Walsh, A., Kovalenko, M. V. Nanocrystals of Cesium Lead Halide Perovskites ($CsPbX_3$, X = Cl, Br, and I): Novel Optoelectronic Materials Showing Bright Emission with Wide Color Gamut. *Nano Lett.* **2015**, *15*, 3692-3696.
7. Zhong, H., Zhou, Y., Ye, M., He, Y., Ye, J., He, C., Yang, C., Li, Y. Controlled Synthesis and Optical Properties of Colloidal Ternary Chalcogenide $CuInS_2$ Nanocrystals. *Chem. Mater.* **2008**, *20*, 6434-6443.
8. Zilevu, D., Creutz, S. E. Shape-Controlled Synthesis of Colloidal Nanorods and Nanoparticles of Barium Titanium Sulfide. *Chem. Mater.* **2021**, *33*, 5137-5146.
9. Boles, M. A., Ling, D., Hyeon, T., Talapin, D. V. The Surface Science of Nanocrystals. *Nat. Mat.* **2016**, *15*, 141-153.
10. Hines, D. A., Kamat, P. V. Recent Advances in Quantum Dot Surface Chemistry. *ACS Appl. Mater. Interfac.* **2014**, *6*, 3041-3057.
11. Kamat, P. V. Semiconductor Surface Chemistry as Holy Grail in Photocatalysis and Photovoltaics. *Acc. Chem. Res.* **2017**, *50*, 527-531.
12. Green, M. L. H. A New Approach to the Formal Classification of Covalent Compounds of the Elements. *J. Organomet. Chem.* **1995**, *500*, 127-148.
13. Anderson, N. C., Hendricks, M. P., Choi, J. J., Owen, J. S. Ligand Exchange and the Stoichiometry of Metal Chalcogenide Nanocrystals: Spectroscopic Observation of Facile Metal-Carboxylate Displacement and Binding. *J. Am. Chem. Soc.* **2013**, *135*, 18536-18548.
14. Owen, J. The Coordination Chemistry of Nanocrystal Surfaces. *Science* **2015**, *347*, 615-616.
15. Nag, A., Kovalenko, M. V., Lee, J.-S., Liu, W., Spokoyny, B., Talapin, D. V. Metal-free Inorganic Ligands for Colloidal Nanocrystals: S^{2-}, HS^-, Se^{2-}, HSe^-, Te^{2-}, HTe^-, TeS_3^{2-}, OH^-, and NH_2^- as Surface Ligands. *J. Am. Chem. Soc.* **2011**, *133*, 10612-10620.

16. Giansante, C., Infante, I., Fabiano, E., Grisorio, R., Suranna, G. P., Gigli, G. "Darker-than-Black" PbS Quantum Dots: Enhancing Optical Absorption of Colloidal Semiconductor Nanocrystals via Short Conjugated Ligands. *J. Am. Chem. Soc.* **2015**, *137*, 1875-1886.
17. Westmoreland, D. E., Lopez-Arteaga, R., Weiss, E. A. N-Heterocyclic Carbenes as Reversible Exciton-Delocalizing Ligands for Photoluminescent Quantum Dots. *J. Am. Chem. Soc.* **2020**, *142*, 2690-2696.
18. De Roo, J., Ibáñez, M., Geiregat, P., Nedelcu, G., Walravens, W., Maes, J., Martins, J. C., Van Driessche, I., Kovalenko, M. V., Hens, Z. Highly Dynamic Ligand Binding and Light Absorption Coefficient of Cesium Lead Bromide Perovskite Nanocrystals. *ACS Nano* **2016**, *10*, 2071-2081.
19. Fritzinger, B., Moreels, I., Lommens, P., Koole, R., Hens, Z., Martins, J. C. In Situ Observation of Rapid Ligand Exchange in Colloidal Nanocrystal Suspensions Using Transfer NOE Nuclear Magnetic Resonance Spectroscopy. *J. Am. Chem. Soc.* **2009**, *131*, 3024-3032.
20. Hartley, C. L., Kessler, M. L., Dempsey, J. L. Molecular-Level Insight into Semiconductor Nanocrystal Surfaces. *J. Am. Chem. Soc.* **2021**, *143*, 1251-1266.
21. Ingole, P. P. A Consolidated Account of Electrochemical Determination of Band Structure Parameters in II–VI Semiconductor Quantum Dots: a Tutorial Review. *Phys. Chem. Chem. Phys.* **2019**, *21*, 4695-4716.
22. Sarma, D. D., Santra, P. K., Mukherjee, S., Nag, A. X-ray Photoelectron Spectroscopy: A Unique Tool To Determine the Internal Heterostructure of Nanoparticles. *Chem. Mater.* **2013**, *25*, 1222-1232.
23. Weber, M., Westendorf, S., Märker, B., Braun, K., Scheele, M. Opportunities and Challenges for Electrochemistry in Studying the Electronic Structure of Nanocrystals. *Phys. Chem. Chem. Phys.* **2019**, *21*, 8992-9001.
24. Li, T., Dief, E. M., Lyu, X., Rahpeima, S., Ciampi, S., Darwish, N. Nanoscale Silicon Oxide Reduces Electron Transfer Kinetics of Surface-Bound Ferrocene Monolayers on Silicon. *J. Phys. Chem. C* **2021**, *125*, 27763-27770.
25. Williams, R. Becquerel Photovoltaic Effect in Binary Compounds. *J. Chem. Phys.* **1960**, *32*, 1505-1514.
26. Berghe, R. A. L. V., Gomes, W. P., Cardon, F. Electrochemical Reactions at the Illuminated CdSe Anode. **1974**, *92*, 91-100.
27. Meissner, D., Benndorf, C., Memming, R. Photocorrosion of Cadmium Sulfide: Analysis by Photoelectron Spectroscopy. *Appl. Surf. Sci.* **1987**, *27*, 423-436.
28. Dworschak, D., Brunnhofer, C., Valtiner, M. Photocorrosion of ZnO Single Crystals during Electrochemical Water Splitting. *ACS Appl. Mater. Interfac.* **2020**, *12*, 51530-51536.
29. Knöppel, J., Kormányos, A., Mayerhöfer, B., Hofer, A., Bierling, M., Bachmann, J., Thiele, S., Cherevko, S. Photocorrosion of WO_3 Photoanodes in Different Electrolytes. *ACS Phys. Chem Au* **2021**, *1*, 6-13.
30. Bard, A. J., Bocarsly, A. B., Fan, F. R. F., Walton, E. G., Wrighton, M. S. The Concept of Fermi Level Pinning at Semiconductor/Liquid Junctions. Consequences for Energy Conversion Efficiency and Selection of Useful Solution Redox Couples in Solar Devices. *J. Am. Chem. Soc.* **1980**, *102*, 3671-3677.

31. Wrighton, M. S., Austin, R. G., Bocarsly, A. B., Bolts, J. M., Haas, O., Legg, K. D., Nadjo, L., Palazzoto, M. C. Design and Study of a Photosensitive Interface: A Derivatized n-Type Silicon Photoelectrode. *J. Am. Chem. Soc.* **1978**, *100*, 1602-1603.
32. Bolts, J. M., Wrighton, M. S. Chemically Derivatized n-Type Semiconducting Germanium Photoelectrodes. Persistent Attachment and Photoelectrochemical Activity of Ferrocene Derivatives. *J. Am. Chem. Soc.* **1978**, *100*, 5257-5262.
33. Bolts, J. M., Bocarsly, A. B., Palazzotto, M. C., Walton, E. G., Lewis, N. S., Wrighton, M. S. Chemically Derivatized n-Type Silicon Photoelectrodes. Stabilization to Surface Corrosion in Aqueous Electrolyte Solutions and Mediation of Oxidation Reactions by Surface-Attached Electroactive Ferrocene Reagents. *J. Am. Chem. Soc.* **1979**, *101*, 1378-1385.
34. Ellis, A. B., Kaiser, S. W., Wrighton, M. S. Visible Light to Electrical Energy Conversion. Stable Cadmium Sulfide and Cadmium Selenide Photoelectrodes in Aqueous Electrolytes. *J. Am. Chem. Soc.* **1976**, *98*, 1635-1637.
35. Rubin, H.-D., Humphrey, B. D., Bocarsly, A. B. Role of Surface Reactions in the Stabilization of n-CdS-Based Photoelectrochemical Cells. *Nature* **1984**, *308*, 339-341.
36. Nasir, J. A., Rehman, Z. u., Shah, S. N. A., Khan, A., Butler, I. S., Catlow, C. R. A. Recent Developments and Perspectives in CdS-Based Photocatalysts for Water Splitting. *J. Mater. Chem. A* **2020**, *8*, 20752-20780.
37. Yu, J. G., Zhang, J., Jaroniec, M. Preparation and Enhanced Visible-Light Photocatalytic H_2-Production Activity of CdS Quantum Dots-Sensitized $Zn_{1-x}Cd_xS$ Solid Solution. *Green Chem.* **2010**, *12*, 1611-1614.
38. Shangguan, W. F., Yoshida, A. Photocatalytic Hydrogen Evolution from Water on Nanocomposites Incorporating Cadmium Sulfide into the Interlayer. *J. Phys. Chem. B* **2002**, *106*, 12227-12230.
39. Zong, X., Yan, H. J., Wu, G. P., Ma, G. J., Wen, F. Y., Wang, L., Li, C. Enhancement of Photocatalytic H_2 Evolution on CdS by Loading MoS_2 as Cocatalyst under Visible Light Irradiation. *J. Am. Chem. Soc.* **2008**, *130*, 7176-7177.
40. Choi, H., Nicolaescu, R., Paek, S., Ko, J., Kamat, P. V. Supersensitization of CdS Quantum Dots with a Near-Infrared Organic Dye: Toward the Design of Panchromatic Hybrid-Sensitized Solar Cells. *ACS Nano* **2011**, *5*, 9238-9245.
41. Buhbut, S., Itzhakov, S., Tauber, E., Shalom, M., Hod, I., Geiger, T., Garini, Y., Oron, D., Zaban, A. Built-in Quantum Dot Antennas in Dye-Sensitized Solar Cells. *ACS Nano* **2010**, *4*, 1293-1298.
42. Korgel, B. A., Monbouquette, H. G. Quantum Confinement Effects Enable Photocatalyzed Nitrate Reduction at Neutral pH Using CdS Nanocrystals. *J. Phys. Chem. B* **1997**, *101*, 5010-5017.
43. Vučemilović, M. I., Vukelić, N., Rajh, T. Solubility and Photocorrosion of Small CdS Particles. *J. Photochem. Photobiol A* **1988**, *42*, 157-167.
44. Sykora, M., Koposov, A. Y., McGuire, J. A., Schulze, R. K., Tretiak, O., Pietryga, J. M., Klimov, V. I. Effect of Air Exposure on Surface Properties, Electronic Structure, and Carrier Relaxation in PbSe Nanocrystals. *ACS Nano* **2010**, *4*, 2021-2034.
45. Yeh, C.-W., Chen, G.-H., Ho, S.-J., Chen, H.-S. Inhibiting the Surface Oxidation of Low-Cadmim-Content ZnS:(Cd,Se) Quantum Dots for Enhancing Application Reliability. *ACS Appl. Nano Mater.* **2019**, *2*, 5290-5301.

46. Cant, D. J. H., Syres, K. L., Lunt, P. J. B., Radtke, H., Treacy, J., Thomas, P. J., Lewis, E. A., Haigh, S. J., O'Brien, P., Schulte, K., Bondino, F., Magnano, E., Flavell, W. R. Surface Properties of Nanocrystalline PbS Films Deposited at the Water–Oil Interface: A Study of Atmospheric Aging. *Langmuir* **2015**, *31*, 1445-1453.
47. Werthen, J. G., Häring, J. P., Bube, R. H. Correlation Between Cadmium Telluride Surface Oxidation and Metal Junctions. *J. Appl. Phys.* **1983**, *54*, 1159-1161.
48. Tang, X., van Welzenis, R. G., van Setten, F. M., Bosch, A. J. Oxidation of the InSb Surface at Room Temperature. *Semicond. Sci. Technol.* **1986**, *1*, 355-365.
49. Surdu-Bob, C. C., Saied, S. O., Sullivan, J. L. An X-ray Photoelectron Spectroscopy Study of the Oxides of GaAs. *Appl. Surf. Sci.* **2001**, *183*, 126-136.
50. Yashina, L. V., Zyubina, T. S., Puttner, R., Zyubin, A. S., Shtanov, V. I., Tikhonov, E. V. A Combined Photoelectron Spectroscopy and ab Initio Study of the Adsorbate System O_2/PbTe(001) and the Oxide Layer Growth Kinetics. *J. Phys. Chem. C* **2008**, *112*, 19995-20006.
51. Mizokawa, Y., Komoda, O., Miyase, S. Long-Time Air Oxidation and Oxide Substrate Reactions on GaSb, GaAs and GaP at Room-Temperature Studied by X-Ray Photoelectron Spectroscopy. *Thin Solid Films* **1988**, *156*, 127-143.
52. Guzelian, A. A., Katari, J. E. B., Kadavanich, A. V., Banin, U., Hamad, K., Juban, E., Alivisatos, A. P., Wolters, R. H., Arnold, C. C., Heath, J. R. Synthesis of Size-Selected, Surface-Passivated InP Nanocrystals. *J. Phys. Chem.* **1996**, *100*, 7212-7219.
53. Katari, J. E. B., Colvin, V. L., Alivisatos, A. P. X-ray Photoelectron Spectroscopy of CdSe Nanocrystals with Applications to Studies of the Nanocrystal Surface. *J. Phys. Chem.* **1994**, *98*, 4109-4117.
54. Hines, D. A., Becker, M. A., Kamat, P. V. Photoinduced Surface Oxidation and Its Effect on the Exciton Dynamics of CdSe Quantum Dots. *J. Phys. Chem. C* **2012**, *116*, 13452-13457.
55. Cheng, L., Xiang, Q., Liao, Y., Zhang, H. CdS-Based Photocatalysts. *Energy Env. Sci.* **2018**, *11*, 1362-1391.
56. Tariq, M., Koch, M. D., Andrews, J. W., Knowles, K. E. Correlation between Surface Chemistry and Optical Properties in Colloidal Cu_2O Nanoparticles. *J. Phys. Chem. C* **2020**, *124*, 4810-4819.
57. Gratzel, M., *Heterogeneous Photochemical Electron Transfer*. CRC Press: Boca Raton, 1989.
58. Wood, A., Giersig, M., Mulvaney, P. Fermi Level Equilibration in Quantum Dot−Metal Nanojunctions. *J. Phys. Chem. B* **2001**, *105*, 8810-8815.
59. Chakrapani, V., Baker, D., Kamat, P. V. Understanding the Role of the Sulfide Redox Couple (S^{2-}/S_n^{2-}) in Quantum Dot-Sensitized Solar Cells. *J. Am. Chem. Soc.* **2011**, *133*, 9607-9615.
60. Kamat, P. V. Boosting the Efficiency of Quantum Dot Sensitized Solar Cells through Modulation of Interfacial Charge Transfer. *Acc. Chem. Res.* **2012**, *45*, 1906-1915.
61. Won, Y.-H., Cho, O., Kim, T., Chung, D.-Y., Kim, T., Chung, H., Jang, H., Lee, J., Kim, D., Jang, E. Highly Efficient and Stable InP/ZnSe/ZnS Quantum Dot Light-Emitting Diodes. *Nature* **2019**, *575*, 634-638.
62. Hu, Z., Liu, S., Qin, H., Zhou, J., Peng, X. Oxygen Stabilizes Photoluminescence of CdSe/CdS Core/Shell Quantum Dots via Deionization. *J. Am. Chem. Soc.* **2020**, *142*, 4254-4264.

63. Shim, M., Guyot-Sionnest, P. n-Type Colloidal Semiconductor Nanocrystals. *Nature* **2000**, *407*, 981-983.
64. Hartley, C. L., Dempsey, J. L. Electron-Promoted X-Type Ligand Displacement at CdSe Quantum Dot Surfaces. *Nano Lett.* **2019**, *19*, 1151-1157.
65. Hartley, C. L., Dempsey, J. L. Revealing the Molecular Identity of Defect Sites on PbS Quantum Dot Surfaces with Redox-Active Chemical Probes. *Chem. Mater.* **2021**, *33*, 2655-2665.
66. Koh, W.-k., Koposov, A. Y., Stewart, J. T., Pal, B. N., Robel, I., Pietryga, J. M., Klimov, V. I. Heavily Doped n-Type PbSe and PbS Nanocrystals Using Ground-State Charge Transfer from Cobaltocene. *Sci. Rep.* **2013**, *3*, 2004.
67. Connelly, N. G., Geiger, W. E. Chemical Redox Agents for Organometallic Chemistry. *Chem. Rev.* **1996**, *96*, 877-910.
68. Rinehart, J. D., Schimpf, A. M., Weaver, A. L., Cohn, A. W., Gamelin, D. R. Photochemical Electronic Doping of Colloidal CdSe Nanocrystals. *J. Am. Chem. Soc.* **2013**, *135*, 18782-18785.
69. Schimpf, A. M., Gunthardt, C. E., Rinehart, J. D., Mayer, J. M., Gamelin, D. R. Controlling Carrier Densities in Photochemically Reduced Colloidal ZnO Nanocrystals: Size Dependence and Role of the Hole Quencher. *J. Am. Chem. Soc.* **2013**, *135*, 16569-16577.
70. van der Stam, W., du Fossé, I., Grimaldi, G., Monchen, J. O. V., Kirkwood, N., Houtepen, A. J. Spectroelectrochemical Signatures of Surface Trap Passivation on CdTe Nanocrystals. *Chem. Mater.* **2018**, *30*, 8052-8061.
71. Ashokan, A., Mulvaney, P. Spectroelectrochemistry of Colloidal CdSe Quantum Dots. *Chem. Mater.* **2021**, *33*, 1353-1362.
72. Tsui, E. Y., Hartstein, K. H., Gamelin, D. R. Selenium Redox Reactivity on Colloidal CdSe Quantum Dot Surfaces. *J. Am. Chem. Soc.* **2016**, *138*, 11105-11108.
73. Rinehart, J. D., Weaver, A. L., Gamelin, D. R. Redox Brightening of Colloidal Semiconductor Nanocrystals Using Molecular Reductants. *J. Am. Chem. Soc.* **2012**, *134*, 16175-16177.
74. Weaver, A. L., Gamelin, D. R. Photoluminescence Brightening via Electrochemical Trap Passivation in ZnSe and Mn^{2+}-Doped ZnSe Quantum Dots. *J. Am. Chem. Soc.* **2012**, *134*, 6819-6825.
75. Wang, C., Shim, M., Guyot-Sionnest, P. Electrochromic Nanocrystal Quantum Dots. *Science* **2001**, *291*, 2390-2392.
76. Shim, M., Wang, C., Guyot-Sionnest, P. Charge-Tunable Optical Properties in Colloidal Semiconductor Nanocrystals. *J. Phys. Chem. B* **2001**, *105*, 2369-2373.
77. Gooding, A. K., Gómez, D. E., Mulvaney, P. The Effects of Electron and Hole Injection on the Photoluminescence of CdSe/CdS/ZnS Nanocrystal Monolayers. *ACS Nano* **2008**, *2*, 669-676.
78. Gong, K., Kelley, D. F. Surface Charging and Trion Dynamics in CdSe-Based Core/Shell Quantum Dots. *J. Phys. Chem. C* **2015**, *119*, 9637-9645.
79. Zeng, Y., Kelley, D. F. Surface Charging in CdSe Quantum Dots: Infrared and Transient Absorption Spectroscopy. *J. Phys. Chem. C* **2017**, *121*, 16657-16664.
80. Zhang, W., Chen, X., Ma, Y., Xu, Z., Wu, L., Yang, Y., Tsang, S.-W., Chen, S. Positive Aging Effect of ZnO Nanoparticles Induced by Surface Stabilization. *J. Phys. Chem. Lett.* **2020**, *11*, 5863-5870.

81. Underwood, D. F., Kippeny, T., Rosenthal, S. J. Ultrafast Carrier Dynamics in CdSe Nanocrystals Determined by Femtosecond Fluorescence Upconversion Spectroscopy. *J. Phys. Chem. B* **2001**, *105*, 436-443.
82. Spanhel, L., Haase, M., Weller, H., Henglein, A. Photochemistry of Colloidal Semiconductors. 20. Surface Modification and Stability of Strong Luminescing CdS Particles. *J. Am. Chem. Soc.* **1987**, *109*, 5649-5655.
83. Norberg, N. S., Gamelin, D. R. Influence of Surface Modification on the Luminescence of Colloidal ZnO Nanocrystals. *J. Phys. Chem. B* **2005**, *109*, 20810-20816.
84. Bohle, D. S., Spina, C. J. The Relationship of Oxygen Binding and Peroxide Sites and the Fluorescent Properties of Zinc Oxide Semiconductor Nanocrystals. *J. Am. Chem. Soc.* **2007**, *129*, 12380-12381.
85. Kippeny, T. C., II, M. J. B., III, A. D. D., McBride, J. R., Orndorff, R. L., Garrett, M. D., Rosenthal, S. J. Effects of Surface Passivation on the Exciton Dynamics of CdSe Nanocrystals as Observed by Ultrafast Fluorescence Upconversion Spectroscopy. *J. Chem. Phys.* **2008**, *128*, 084713.
86. Manna, L., Scher, E. C., Li, L.-S., Alivisatos, A. P. Epitaxial Growth and Photochemical Annealing of Graded CdS/ZnS Shells on Colloidal CdSe Nanorods. *J. Am. Chem. Soc.* **2002**, *124*, 7136-7145.
87. Jones, M., Nedeljkovic, J., Ellingson, R. J., Nozik, A. J., Rumbles, G. Photoenhancement of Luminescence in Colloidal CdSe Quantum Dot Solutions. *J. Phys. Chem. B* **2003**, *107*, 11346-11352.
88. Asami, H., Abe, Y., Ohtsu, T., Kamiya, I., Hara, M. Surface State Analysis of Photobrightening in CdSe Nanocrystal Thin Films. *J. Phys. Chem. B* **2003**, *107*, 12566-12568.
89. Cordero, S. R., Carson, P. J., Estabrook, R. A., Strouse, G. F., Buratto, S. K. Photo-Activated Luminescence of CdSe Quantum Dot Monolayers. *J. Phys. Chem. B* **2000**, *104*, 12137-12142.
90. Nazzal, A. Y., Wang, X., Qu, L., Yu, W., Wang, Y., Peng, X., Xiao, M. Environmental Effects on Photoluminescence of Highly Luminescent CdSe and CdSe/ZnS Core/Shell Nanocrystals in Polymer Thin Films. *J. Phys. Chem. B* **2004**, *108*, 5507-5515.
91. Lee, S. F., Osborne, M. A. Photodynamics of a Single Quantum Dot: Fluorescence Activation, Enhancement, Intermittency, and Decay. *J. Am. Chem. Soc.* **2007**, *129*, 8936-8937.
92. Peterson, J. J., Krauss, T. D. Photobrightening and Photodarkening in PbS Quantum Dots. *Phys. Chem. Chem. Phys.* **2006**, *8*, 3851-3856.
93. Chen, P.-R., Lai, K.-Y., Chen, H.-S. Roles of Alcohols and Existing Metal Ions in Surface Chemistry and Photoluminescence of InP Cores. *Mater. Adv.* **2021**, *2*, 6039-6048.
94. Inoue, K., Kojima, T., Sugimoto, H., Fujii, M. Charge Transfer-Induced Photobrightening of Silicon Quantum Dots in Water Containing a Molecular Reductant. *J. Phys. Chem. C* **2019**, *123*, 1512-1518.
95. Jasieniak, J., Mulvaney, P. From Cd-Rich to Se-Rich − the Manipulation of CdSe Nanocrystal Surface Stoichiometry. *J. Am. Chem. Soc.* **2007**, *129*, 2841-2848.
96. Krivenkov, V., Samokhvalov, P., Zvaigzne, M., Martynov, I., Chistyakov, A., Nabiev, I. Ligand-Mediated Photobrightening and Photodarkening of CdSe/ZnS Quantum Dot Ensembles. *J. Phys. Chem. C* **2018**, *122*, 15761-15771.

97. Myung, N., Bae, Y., Bard, A. J. Enhancement of the Photoluminescence of CdSe Nanocrystals Dispersed in $CHCl_3$ by Oxygen Passivation of Surface States. *Nano Lett.* **2003**, *3*, 747-749.
98. Kusterer, R., Ruhmlieb, C., Strelow, C., Kipp, T., Mews, A. Reversible and Irreversible Effects of Oxygen on the Optical Properties of CdSe Quantum Wires. *J. Phys. Chem. C* **2022**, *126*, 19240-19249.
99. Gómez, D. E., van Embden, J., Jasieniak, J., Smith, T. A., Mulvaney, P. Blinking and Surface Chemistry of Single CdSe Nanocrystals. *Small* **2006**, *2*, 204-208.
100. Galland, C., Ghosh, Y., Steinbrück, A., Sykora, M., Hollingsworth, J. A., Klimov, V. I., Htoon, H. Two Types of Luminescence Blinking Revealed by Spectroelectrochemistry of Single Quantum Dots. *Nature* **2011**, *479*, 203-207.
101. Empedocles, S. A., Bawendi, M. G. Quantum-Confined Stark Effect in Single CdSe Nanocrystallite Quantum Dots. *Science* **1997**, *278*, 2114-2117.
102. Empedocles, S. A., Bawendi, M. G. Influence of Spectral Diffusion on the Line Shapes of Single CdSe Nanocrystallite Quantum Dots. *J. Phys. Chem. B* **1999**, *103*, 1826-1830.
103. Aldana, J., Wang, Y. A., Peng, X. Photochemical Instability of CdSe Nanocrystals Coated by Hydrophilic Thiols. *J. Am. Chem. Soc.* **2001**, *123*, 8844-8850.
104. Buckley, J. J., Couderc, E., Greaney, M. J., Munteanu, J., Riche, C. T., Bradforth, S. E., Brutchey, R. L. Chalcogenol Ligand Toolbox for CdSe Nanocrystals and Their Influence on Exciton Relaxation Pathways. *ACS Nano* **2014**, *8*, 2512-2521.
105. Munro, A. M., Ginger, D. S. Photoluminescence Quenching of Single CdSe Nanocrystals by Ligand Adsorption. *Nano Lett.* **2008**, *8*, 2585-2590.
106. Koberling, F., Mews, A., Basché, T. Oxygen-Induced Blinking of Single CdSe Nanocrystals. *Adv. Mater.* **2001**, *13*, 672-676.
107. Müller, J., Lupton, J. M., Rogach, A. L., Feldmann, J., Talapin, D. V., Weller, H. Air-Induced Fluorescence Bursts from Single Semiconductor Nanocrystals. *Appl. Phys. Lett.* **2004**, *85*, 381-383.
108. Zhao, J., Holmes, M. A., Osterloh, F. E. Quantum Confinement Controls Photocatalysis: A Free Energy Analysis for Photocatalytic Proton Reduction at CdSe Nanocrystals. *ACS Nano* **2013**, *7*, 4316-4325.
109. Gutiérrez, M., Henglein, A. Photochemistry of Colloidal Metal Sulfides. 4. Cathodic Dissolution of CdS and Excess Cd^{2+} Reduction. *Ber. Bunsenges. Phys. Chem.* **1983**, *87*, 474-478.
110. Houtepen, A. J., Hens, Z., Owen, J. S., Infante, I. On the Origin of Surface Traps in Colloidal II–VI Semiconductor Nanocrystals. *Chem. Mater.* **2017**, *29*, 752-761.
111. du Fossé, I., ten Brinck, S., Infante, I., Houtepen, A. J. Role of Surface Reduction in the Formation of Traps in n-Doped II–VI Semiconductor Nanocrystals: How to Charge without Reducing the Surface. *Chem. Mater.* **2019**, *31*, 4575-4583.
112. Voznyy, O., Thon, S. M., Ip, A. H., Sargent, E. H. Dynamic Trap Formation and Elimination in Colloidal Quantum Dots. *J. Phys. Chem. Lett.* **2013**, *4*, 987-992.
113. du Fossé, I., Boehme, S. C., Infante, I., Houtepen, A. J. Dynamic Formation of Metal-Based Traps in Photoexcited Colloidal Quantum Dots and Their Relevance for Photoluminescence. *Chem. Mater.* **2021**, *33*, 3349-3358.
114. Imada, Y., Nakano, H., Furukawa, K., Kishi, R., Nakano, M., Maruyama, H., Nakamoto, M., Sekiguchi, A., Ogawa, M., Ohta, T., Yamamoto, Y. Isolation of Hypervalent Group-

16 Radicals and Their Application in Organic-Radical Batteries. *J. Am. Chem. Soc.* **2016**, *138*, 479-482.
115. Wu, Q., Zhang, T., Geng, J., Gao, S., Ma, H., Li, F. Anionic Redox Chemistry for Sodium-Ion Batteries: Mechanisms, Advances, and Challenges. *Energy & Fuels* **2022**, *36*, 8081-8095.
116. Ubbink, R. F., Almeida, G., Iziyi, H., du Fossé, I., Verkleij, R., Ganapathy, S., van Eck, E. R. H., Houtepen, A. J. A Water-Free In Situ HF Treatment for Ultrabright InP Quantum Dots. *Chem. Mater.* **2022**, *34*, 10093-10103.
117. Li, Y., Xu, X., Wang, C., Ecker, B., Yang, J., Huang, J., Gao, Y. Light-Induced Degradation of $CH_3NH_3PbI_3$ Hybrid Perovskite Thin Film. *J. Phys. Chem. C* **2017**, *121*, 3904-3910.
118. Kim, G. Y., Senocrate, A., Yang, T.-Y., Gregori, G., Grätzel, M., Maier, J. Large Tunable Photoeffect on Ion Conduction in Halide Perovskites and Implications for Photodecomposition. *Nat. Mat.* **2018**, *17*, 445-449.
119. Xian, L., Zhang, X., Li, X. Voltammetric Determination of Electronic Structure of Quantum Dots. *Curr. Opin. Electrochem.* **2022**, *34*, 101022.
120. Haram, S. K., Quinn, B. M., Bard, A. J. Electrochemistry of CdS Nanoparticles: A Correlation between Optical and Electrochemical Band Gaps. *J. Am. Chem. Soc.* **2001**, *123*, 8860-8861.
121. Chen, S., Truax, L. A., Sommers, J. M. Alkanethiolate-Protected PbS Nanoclusters: Synthesis, Spectroscopic and Electrochemical Studies. *Chem. Mater.* **2000**, *12*, 3864-3870.
122. Bae, Y., Myung, N., Bard, A. J. Electrochemistry and Electrogenerated Chemiluminescence of CdTe Nanoparticles. *Nano Lett.* **2004**, *4*, 1153-1161.
123. Jin, L., Shang, L., Zhai, J., Li, J., Dong, S. Fluorescence Spectroelectrochemistry of Multilayer Film Assembled CdTe Quantum Dots Controlled by Applied Potential in Aqueous Solution. *J. Phys. Chem. C* **2010**, *114*, 803-807.
124. Liu, J., Yang, W., Li, Y., Fan, L., Li, Y. Electrochemical Studies of the Effects of the Size, Ligand and Composition on the Band Structures of CdSe, CdTe and Their Alloy Nanocrystals. *Phys. Chem. Chem. Phys.* **2014**, *16*, 4778-4788.
125. Poznyak, S. K., Osipovich, N. P., Shavel, A., Talapin, D. V., Gao, M., Eychmüller, A., Gaponik, N. Size-Dependent Electrochemical Behavior of Thiol-Capped CdTe Nanocrystals in Aqueous Solution. *J. Phys. Chem. B* **2005**, *109*, 1094-1100.
126. Amelia, M., Impellizzeri, S., Monaco, S., Yildiz, I., Silvi, S., Raymo, F. M., Credi, A. Structural and Size Effects on the Spectroscopic and Redox Properties of CdSe Nanocrystals in Solution: The Role of Defect States. *ChemPhysChem* **2011**, *12*, 2280-2288.
127. Ingole, P. P., Markad, G. B., Saraf, D., Tatikondewar, L., Nene, O., Kshirsagar, A., Haram, S. K. Band Gap Bowing at Nanoscale: Investigation of CdS_xSe_{1-x} Alloy Quantum Dots through Cyclic Voltammetry and Density Functional Theory. *J. Phys. Chem. C* **2013**, *117*, 7376-7383.
128. Kucur, E., Riegler, J., Urban, G. A., Nann, T. Determination of Quantum Confinement in CdSe Nanocrystals by Cyclic Voltammetry. *J. Chem. Phys.* **2003**, *119*, 2333-2337.
129. Greaney, M. J., Couderc, E., Zhao, J., Nail, B. A., Mecklenburg, M., Thornbury, W., Osterloh, F. E., Bradforth, S. E., Brutchey, R. L. Controlling the Trap State Landscape of

Colloidal CdSe Nanocrystals with Cadmium Halide Ligands. *Chem. Mater.* **2015**, *27*, 744-756.
130. de la Cueva, L., Lauwaet, K., Otero, R., Gallego, J. M., Alonso, C., Juarez, B. H. Effect of Chloride Ligands on CdSe Nanocrystals by Cyclic Voltammetry and X-ray Photoelectron Spectroscopy. *J. Phys. Chem. C* **2014**, *118*, 4998-5004.
131. Elgrishi, N., Rountree, K. J., McCarthy, B. D., Rountree, E. S., Eisenhart, T. T., Dempsey, J. L. A Practical Beginner's Guide to Cyclic Voltammetry. *J. Chem. Educ.* **2018**, *95*, 197-206.
132. Homer, M. K., Kuo, D.-Y., Dou, F. Y., Cossairt, B. M. Photoinduced Charge Transfer from Quantum Dots Measured by Cyclic Voltammetry. *J. Am. Chem. Soc.* **2022**, *144*, 14226-14234.
133. Kronik, L., Shapira, Y. Surface Photovoltage Phenomena: Theory, Experiment, and Applications. *Surf. Sci. Rep.* **1999**, *37*, 1-206.
134. Zhao, J., Nail, B. A., Holmes, M. A., Osterloh, F. E. Use of Surface Photovoltage Spectroscopy to Measure Built-in Voltage, Space Charge Layer Width, and Effective Band Gap in CdSe Quantum Dot Films. *J. Phys. Chem. Lett.* **2016**, *7*, 3335-3340.
135. Muthuswamy, E., Zhao, J., Tabatabaei, K., Amador, M. M., Holmes, M. A., Osterloh, F. E., Kauzlarich, S. M. Thiol-Capped Germanium Nanocrystals: Preparation and Evidence for Quantum Size Effects. *Chem. Mater.* **2014**, *26*, 2138-2146.
136. Wang, S., Zhang, J., Gharbi, O., Vivier, V., Gao, M., Orazem, M. E. Electrochemical Impedance Spectroscopy. *Nat. Rev. Methods Primers* **2021**, *1*, 41.
137. Brewster, D. A., Koch, M. D., Knowles, K. E. Evaluation of Electrochemical Properties of Nanostructured Metal Oxide Electrodes Immersed in Redox-Inactive Organic Media. *Phys. Chem. Chem. Phys.* **2021**, *23*, 17904-17916.
138. Volk, S., Yazdani, N., Sanusoglu, E., Yarema, O., Yarema, M., Wood, V. Measuring the Electronic Structure of Nanocrystal Thin Films Using Energy-Resolved Electrochemical Impedance Spectroscopy. *J. Phys. Chem. Lett.* **2018**, *9*, 1384-1392.
139. Volk, S., Yazdani, N., Yarema, O., Yarema, M., Wood, V. Dopants and Traps in Nanocrystal-Based Semiconductor Thin Films: Origins and Measurement of Electronic Midgap States. *ACS Appl. Electron. Mater.* **2020**, *2*, 398-404.
140. Osipovich, N. P., Shavel, A., Poznyak, S. K., Gaponik, N., Eychmüller, A. Electrochemical Observation of the Photoinduced Formation of Alloyed ZnSe(S) Nanocrystals. *J. Phys. Chem. B* **2006**, *110*, 19233-19237.
141. Wang, F., Tang, R., Buhro, W. E. The Trouble with TOPO; Identification of Adventitious Impurities Beneficial to the Growth of Cadmium Selenide Quantum Dots, Rods, and Wires. *Nano Lett.* **2008**, *8*, 3521-3524.
142. Hens, Z., Martins, J. C. A Solution NMR Toolbox for Characterizing the Surface Chemistry of Colloidal Nanocrystals. *Chem. Mater.* **2013**, *25*, 1211-1221.
143. Hens, Z., Moreels, I., Martins, J. C. In Situ ^{1}H NMR Study on the Trioctylphosphine Oxide Capping of Colloidal InP Nanocrystals. *ChemPhysChem* **2005**, *6*, 2578-2584.
144. Ribot, F., Escax, V., Roiland, C., Sanchez, C., Martins, J. C., Biesemans, M., Verbruggen, I., Willem, R. In Situ Evaluation of Interfacial Affinity in CeO_2 Based Hybrid Nanoparticles by Pulsed Field Gradient NMR. *Chem. Commun.* **2005**, 1019-1021.
145. Fritzinger, B., Capek, R. K., Lambert, K., Martins, J. C., Hens, Z. Utilizing Self-Exchange To Address the Binding of Carboxylic Acid Ligands to CdSe Quantum Dots. *J. Am. Chem. Soc.* **2010**, *132*, 10195-10201.

146. Shen, Y., Gee, M. Y., Tan, R., Pellechia, P. J., Greytak, A. B. Purification of Quantum Dots by Gel Permeation Chromatography and the Effect of Excess Ligands on Shell Growth and Ligand Exchange. *Chem. Mater.* **2013**, *25*, 2838-2848.
147. Anderson, N. C., Owen, J. S. Soluble, Chloride-Terminated CdSe Nanocrystals: Ligand Exchange Monitored by ^{1}H and ^{31}P NMR Spectroscopy. *Chem. Mater.* **2013**, *25*, 69-76.
148. García-Rodríguez, R., Liu, H. Solution Structure of Cadmium Carboxylate and its Implications for the Synthesis of Cadmium Chalcogenide Nanocrystals. *Chem. Commun.* **2013**, *49*, 7857-7859.
149. García-Rodríguez, R., Liu, H. Mechanistic Insights into the Role of Alkylamine in the Synthesis of CdSe Nanocrystals. *J. Am. Chem. Soc.* **2014**, *136*, 1968-1975.
150. Mehring, M., *Principles of High Resolution NMR in Solids*. 2nd ed.; Springer Berlin, Heidelberg: 1983.
151. Tomaselli, M., Yarger, J. L., Jr., M. B., Havlin, R. H., deGraw, D., Pines, A., Alivisatos, A. P. NMR Study of InP Quantum Dots: Surface Structure and Size Effects. *J. Chem. Phys.* **1999**, *110*, 8861-8864.
152. Cros-Gagneux, A., Delpech, F., Nayral, C., Cornejo, A., Coppel, Y., Chaudret, B. Surface Chemistry of InP Quantum Dots: A Comprehensive Study. *J. Am. Chem. Soc.* **2010**, *132*, 18147-18157.
153. Berrettini, M. G., Braun, G., Hu, J. G., Strouse, G. F. NMR Analysis of Surfaces and Interfaces in 2-nm CdSe. *J. Am. Chem. Soc.* **2004**, *126*, 7063-7070.
154. Lovingood, D. D., Achey, R., Paravastu, A. K., Strouse, G. F. Size- and Site-Dependent Reconstruction in CdSe QDs Evidenced by ^{77}Se{^{1}H} CP-MAS NMR Spectroscopy. *J. Am. Chem. Soc.* **2010**, *132*, 3344-3354.
155. De Paëpe, G., Lesage, A., Steuernagel, S., Emsley, L. Transverse Dephasing Optimised NMR Spectroscopy in Solids: Natural-Abundance ^{13}C Correlation Spectra. *ChemPhysChem* **2004**, *5*, 869-875.
156. Li, M., Ouyang, J., Ratcliffe, C. I., Pietri, L., Wu, X., Leek, D. M., Moudrakovski, I., Lin, Q., Yang, B., Yu, K. CdS Magic-Sized Nanocrystals Exhibiting Bright Band Gap Photoemission via Thermodynamically Driven Formation. *ACS Nano* **2009**, *3*, 3832-3838.
157. Chen, Y., Smock, S. R., Flintgruber, A. H., Perras, F. A., Brutchey, R. L., Rossini, A. J. Surface Termination of $CsPbBr_3$ Perovskite Quantum Dots Determined by Solid-State NMR Spectroscopy. *J. Am. Chem. Soc.* **2020**, *142*, 6117-6127.
158. Xing, B., Ge, S., Zhao, J., Yang, H., Song, J., Geng, Y., Qiao, Y., Gu, L., Han, P., Ma, G. Alloyed Crystalline $CdSe_{1-x}S_x$ Semiconductive Nanomaterials – A Solid State ^{113}Cd NMR Study. *ChemistryOpen* **2020**, *9*, 1018-1026.
159. Maly, T., Debelouchina, G. T., Bajaj, V. S., Hu, K.-N., Joo, C.-G., Mak–Jurkauskas, M. L., Sirigiri, J. R., Wel, P. C. A. v. d., Herzfeld, J., Temkin, R. J., Griffin, R. G. Dynamic Nuclear Polarization at High Magnetic Fields. *J. Chem. Phys.* **2008**, *128*, 052211.
160. Ni, Q. Z., Daviso, E., Can, T. V., Markhasin, E., Jawla, S. K., Swager, T. M., Temkin, R. J., Herzfeld, J., Griffin, R. G. High Frequency Dynamic Nuclear Polarization. *Acc. Chem. Res.* **2013**, *46*, 1933-1941.
161. Piveteau, L., Ong, T.-C., Rossini, A. J., Emsley, L., Copéret, C., Kovalenko, M. V. Structure of Colloidal Quantum Dots from Dynamic Nuclear Polarization Surface Enhanced NMR Spectroscopy. *J. Am. Chem. Soc.* **2015**, *137*, 13964-13971.

162. Takahashi, H., Lee, D., Dubois, L., Bardet, M., Hediger, S., De Paëpe, G. Rapid Natural-Abundance 2D ^{13}C–^{13}C Correlation Spectroscopy Using Dynamic Nuclear Polarization Enhanced Solid-State NMR and Matrix-Free Sample Preparation. *Angew. Chem. Int. Ed.* **2012**, *51*, 11766-11769.
163. Chen, Y., Dorn, R. W., Hanrahan, M. P., Wei, L., Blome-Fernández, R., Medina-Gonzalez, A. M., Adamson, M. A. S., Flintgruber, A. H., Vela, J., Rossini, A. J. Revealing the Surface Structure of CdSe Nanocrystals by Dynamic Nuclear Polarization-Enhanced ^{77}Se and ^{113}Cd Solid-State NMR Spectroscopy. *J. Am. Chem. Soc.* **2021**, *143*, 8747-8760.
164. Hanrahan, M. P., Chen, Y., Blome-Fernández, R., Stein, J. L., Pach, G. F., Adamson, M. A. S., Neale, N. R., Cossairt, B. M., Vela, J., Rossini, A. J. Probing the Surface Structure of Semiconductor Nanoparticles by DNP SENS with Dielectric Support Materials. *J. Am. Chem. Soc.* **2019**, *141*, 15532-15546.
165. Mishra, A., Hope, M. A., Almalki, M., Pfeifer, L., Zakeeruddin, S. M., Grätzel, M., Emsley, L. Dynamic Nuclear Polarization Enables NMR of Surface Passivating Agents on Hybrid Perovskite Thin Films. *J. Am. Chem. Soc.* **2022**, *144*, 15175-15184.
166. Roth, A. N., Chen, Y., Adamson, M. A. S., Gi, E., Wagner, M., Rossini, A. J., Vela, J. Alkaline-Earth Chalcogenide Nanocrystals: Solution-Phase Synthesis, Surface Chemistry, and Stability. *ACS Nano* **2022**, *16*, 12024-12035.
167. Watkins, G. D. EPR of Defects in Semiconductors: Past, Present, Future. *Phys. Solid* **1999**, *41*, 746-750.
168. Kakazey, N. G., Sreckovic, T. V., Ristic, M. M. Electronic Paramagnetic Resonance Investigation of the Evolution of Defects in Zinc Oxide During Tribophysical Activation. *J. Mater. Sci.* **1997**, *32*, 4619-4622.
169. eYu, B., Zhu, C., Gan, F., Huang, Y. Electron Spin Resonance Properties of ZnO Microcrystallites. *Mater. Lett.* **1998**, *33*, 247-250.
170. Ischenko, V., Polarz, S., Grote, D., Stavarache, V., Fink, K., Driess, M. Zinc Oxide Nanoparticles with Defects. *Adv. Funct. Mater.* **2005**, *15*, 1945-1954.
171. Kumar, C. P., Gopal, N. O., Wang, T. C., Wong, M.-S., Ke, S. C. EPR Investigation of TiO_2 Nanoparticles with Temperature-Dependent Properties. *J. Phys. Chem. B* **2006**, *110*, 5223-5229.
172. Ipe, B. I., Lehnig, M., Niemeyer, C. M. On the Generation of Free Radical Species from Quantum Dots. *Small* **2005**, *1*, 706-709.
173. Norberg, N. S., Kittilstved, K. R., Amonette, J. E., Kukkadapu, R. K., Schwartz, D. A., Gamelin, D. R. Synthesis of Colloidal Mn^{2+}:ZnO Quantum Dots and High-T_C Ferromagnetic Nanocrystalline Thin Films. *J. Am. Chem. Soc.* **2004**, *126*, 9387-9398.
174. Anitha, B., Khadar, M. A., Banerjee, A. Paramagnetic Behavior of Co Doped TiO_2 Nanocrystals Controlled by Self-Purification Mechanism. *J. Solid State Chem.* **2016**, *239*, 237-245.
175. Blair, M. W., Muenchausen, R. E., Bennett, B. L., Smith, N. A., Warner, M. G. Correlated Spin Systems in Undoped CdSe Quantum Dots. *J. Nanopart. Res.* **2013**, *15*, 1953.
176. Archer, P. I., Santangelo, S. A., Gamelin, D. R. Direct Observation of sp−d Exchange Interactions in Colloidal Mn^{2+}- and Co^{2+}-Doped CdSe Quantum Dots. *Nano Lett.* **2007**, *7*, 1037-1043.

177. Mi, C., Saniepay, M., Beaulac, R. Overcoming the Complex Excited-State Dynamics of Colloidal Cadmium Selenide Nanocrystals Involved in Energy Transfer Processes. *Chem. Mater.* **2018**, *30*, 5714-5725.
178. Dutta, P., Tang, Y., Mi, C., Saniepay, M., McGuire, J. A., Beaulac, R. Ultrafast Hole Extraction from Photoexcited Colloidal CdSe Quantum Dots Coupled to Nitroxide Free Radicals. *J. Chem. Phys.* **2019**, *151*, 174706.
179. Maurel, V., Laferrière, M., Billone, P., Godin, R., Scaiano, J. C. Free Radical Sensor Based on CdSe Quantum Dots with Added 4-Amino-2,2,6,6-Tetramethylpiperidine Oxide Functionality. *J. Phys. Chem. B* **2006**, *110*, 16353-16358.
180. Billone, P. S., Maretti, L., Maurel, V., Scaiano, J. C. Dynamics of the Dissociation of a Disulfide Biradical on a CdSe Nanoparticle Surface. *J. Am. Chem. Soc.* **2007**, *129*, 14150-14151.
181. Liu, W. K., Whitaker, K. M., Smith, A. L., Kittilstved, K. R., Robinson, B. H., Gamelin, D. R. Room-Temperature Electron Spin Dynamics in Free-Standing ZnO Quantum Dots. *Phys. Rev. Lett.* **2007**, *98*, 186804.
182. Wang, Z. L. Characterization of Nanophase Materials. *Particle & Particle Systems Characterization* **2001**, *18*, 142-165.
183. Bertoni, G., Grillo, V., Brescia, R., Ke, X., Bals, S., Catellani, A., Li, H., Manna, L. Direct Determination of Polarity, Faceting, and Core Location in Colloidal Core/Shell Wurtzite Semiconductor Nanocrystals. *ACS Nano* **2012**, *6*, 6453-6461.
184. Ondry, J. C., Hauwiller, M. R., Alivisatos, A. P. Dynamics and Removal Pathway of Edge Dislocations in Imperfectly Attached PbTe Nanocrystal Pairs: Toward Design Rules for Oriented Attachment. *ACS Nano* **2018**, *12*, 3178-3189.
185. Pu, S., Gong, C., Robertson, A. W. Liquid Cell Transmission Electron Microscopy and its Applications. *R. Soc. Open Sci.* **2020**, *7*, 191204.
186. Zheng, H., Claridge, S. A., Minor, A. M., Alivisatos, A. P., Dahmen, U. Nanocrystal Diffusion in a Liquid Thin Film Observed by in Situ Transmission Electron Microscopy. *Nano Lett.* **2009**, *9*, 2460-2465.
187. Evans, J. E., Jungjohann, K. L., Browning, N. D., Arslan, I. Controlled Growth of Nanoparticles from Solution with In Situ Liquid Transmission Electron Microscopy. *Nano Lett.* **2011**, *11*, 2809-2813.
188. Hodnik, N., Dehm, G., Mayrhofer, K. J. J. Importance and Challenges of Electrochemical in Situ Liquid Cell Electron Microscopy for Energy Conversion Research. *Acc. Chem. Res.* **2016**, *49*, 2015-2022.
189. Moreno-Hernandez, I. A., Crook, M. F., Ondry, J. C., Alivisatos, A. P. Redox Mediated Control of Electrochemical Potential in Liquid Cell Electron Microscopy. *J. Am. Chem. Soc.* **2021**, *143*, 12082-12089.
190. Bergmann, A., Roldan Cuenya, B. Operando Insights into Nanoparticle Transformations during Catalysis. *ACS Catal.* **2019**, *9*, 10020-10043.
191. Zhang, J., Zhang, H. B., Cao, W. C., Pang, Z. F., Li, J. Z., Shu, Y. F., Zhu, C. Q., Kong, X. Q., Wang, L. J., Peng, X. G. Identification of Facet-Dependent Coordination Structures of Carboxylate Ligands on CdSe Nanocrystals. *J. Am. Chem. Soc.* **2019**, *141*, 15675-15683.
192. Zhu, C. Q., Chen, D. D., Cao, W. C., Lai, R. C., Pu, C. D., Li, J. Z., Kong, X. Q., Peng, X. G. Facet-Dependent On-Surface Reactions in the Growth of CdSe Nanoplatelets. *Angew. Chem. Int. Ed.* **2019**, *58*, 17764-17770.

193. Hartstein, K. H., Brozek, C. K., Hinterding, S. O. M., Gamelin, D. R. Copper-Coupled Electron Transfer in Colloidal Plasmonic Copper-Sulfide Nanocrystals Probed by in Situ Spectroelectrochemistry. *J. Am. Chem. Soc.* **2018**, *140*, 3434-3442.
194. Schrauben, J. N., Hayoun, R., Valdez, C. N., Braten, M., Fridley, L., Mayer, J. M. Titanium and Zinc Oxide Nanoparticles Are Proton-Coupled Electron Transfer Agents. *Science* **2012**, *336*, 1298-1301.
195. Peper, J. L., Mayer, J. M. Manifesto on the Thermochemistry of Nanoscale Redox Reactions for Energy Conversion. *ACS Energy Lett.* **2019**, *4*, 866-872.
196. Puntambekar, A., Wang, Q., Miller, L., Smieszek, N., Chakrapani, V. Electrochemical Charging of CdSe Quantum Dots: Effects of Adsorption versus Intercalation. *ACS Nano* **2016**, *10*, 10988-10999.
197. Lemon, B. I., Hupp, J. T. Photochemical Quartz Crystal Microbalance Study of the Nanocrystalline Titanium Dioxide Semiconductor Electrode/Water Interface: Simultaneous Photoaccumulation of Electrons and Protons. *J. Phys. Chem.* **1996**, *100*, 14578-14580.
198. Morris-Cohen, A. J., Donakowski, M. D., Knowles, K. E., Weiss, E. A. The Effect of a Common Purification Procedure on the Chemical Composition of the Surfaces of CdSe Quantum Dots Synthesized with Trioctylphosphine Oxide. *J. Phys. Chem. C* **2010**, *114*, 897-906.
199. Morrison, C., Sun, H., Yao, Y., Loomis, R. A., Buhro, W. E. Methods for the ICP-OES Analysis of Semiconductor Materials. *Chem. Mater.* **2020**, *32*, 1760-1768.
200. Kroupa, D. M., Vörös, M., Brawand, N. P., McNichols, B. W., Miller, E. M., Gu, J., Nozik, A. J., Sellinger, A., Galli, G., Beard, M. C. Tuning Colloidal Quantum Dot Band Edge Positions through Solution-Phase Surface Chemistry Modification. *Nat. Commun.* **2017**, *8*, 15257.
201. McNichols, B. W., Koubek, J. T., Sellinger, A. Single-Step Synthesis of Styryl Phosphonic Acids via Palladium-Catalyzed Heck Coupling of Vinyl Phosphonic Acid with Aryl Halides. *Chem. Commun.* **2017**, *53*, 12454-12456.
202. Kovalenko, M. V., Scheele, M., Talapin, D. V. Colloidal Nanocrystals with Molecular Metal Chalcogenide Surface Ligands. *Science* **2009**, *324*, 1417-1420.
203. Nagy, A., Steinbrück, A., Gao, J., Doggett, N., Hollingsworth, J. A., Iyer, R. Comprehensive Analysis of the Effects of CdSe Quantum Dot Size, Surface Charge, and Functionalization on Primary Human Lung Cells. *ACS Nano* **2012**, *6*, 4748-4762.
204. Derjaguin, B., Landau, L. Theory of the Stability of Strongly Charged Lyophobic Sols and of the Adhesion of Strongly Charged Particles in Solutions of Electrolytes. *Prog. Surf. Sci.* **1993**, *43*, 30-59.
205. Clogston, J. D., Patri, A. K. Zeta Potential Measurement. In *Characterization of Nanoparticles Intended for Drug Delivery*, McNeil, S. E., Ed. Humana Press: Totowa, NJ, 2011; pp 63-70.
206. Bhattacharjee, S. DLS and Zeta Potential – What They Are and What They Are Not? *J. Contr. Release* **2016**, *235*, 337-351.
207. Delforce, L., Hofmann, E., Nardello-Rataj, V., Aubry, J.-M. TiO_2 Nanoparticle Dispersions in Water and Nonaqueous Solvents Studied by Gravitational Sedimentation Analysis: Complementarity of Hansen Parameters and DLVO interpretations. *Colloids Surf. A: Physicochem. Eng. Asp.* **2021**, *628*, 127333.

208. Houtepen, A. J., Vanmaekelbergh, D. Orbital Occupation in Electron-Charged CdSe Quantum-Dot Solids. *J. Phys. Chem. B* **2005**, *109*, 19634-19642.
209. Radchanka, A., Hrybouskaya, V., Iodchik, A., Achtstein, A. W., Artemyev, M. Zeta Potential-Based Control of CdSe/ZnS Quantum Dot Photoluminescence. *J. Phys. Chem. Lett.* **2022**, *13*, 4912-4917.
210. Nag, A., Chung, D. S., Dolzhnikov, D. S., Dimitrijevic, N. M., Chattopadhyay, S., Shibata, T., Talapin, D. V. Effect of Metal Ions on Photoluminescence, Charge Transport, Magnetic and Catalytic Properties of All-Inorganic Colloidal Nanocrystals and Nanocrystal Solids. *J. Am. Chem. Soc.* **2012**, *134*, 13604-13615.
211. Sung, Y., Lee, W., Lee, E., Ko, Y. H., Kim, S. Ion-Pair Ligand-Assisted Surface Stoichiometry Control of Ag_2S Nanocrystals. *Chem. Mater.* **2022**, *34*, 9945-9954.
212. Wei, H. H. Y., Evans, C. M., Swartz, B. D., Neukirch, A. J., Young, J., Prezhdo, O. V., Krauss, T. D. Colloidal Semiconductor Quantum Dots with Tunable Surface Composition. *Nano Lett.* **2012**, *12*, 4465-4471.
213. Soreni-Harari, M., Yaacobi-Gross, N., Steiner, D., Aharoni, A., Banin, U., Millo, O., Tessler, N. Tuning Energetic Levels in Nanocrystal Quantum Dots through Surface Manipulations. *Nano Lett.* **2008**, *8*, 678-684.
214. Munro, A. M., Zacher, B., Graham, A., Armstrong, N. R. Photoemission Spectroscopy of Tethered CdSe Nanocrystals: Shifts in Ionization Potential and Local Vacuum Level as a Function of Nanocrystal Capping Ligand. *ACS Appl. Mater. Interfac.* **2010**, *2*, 863-869.
215. Brown, P. R., Kim, D., Lunt, R. R., Zhao, N., Bawendi, M. G., Grossman, J. C., Bulović, V. Energy Level Modification in Lead Sulfide Quantum Dot Thin Films through Ligand Exchange. *ACS Nano* **2014**, *8*, 5863-5872.
216. Santra, P. K., Palmstrom, A. F., Tanskanen, J. T., Yang, N., Bent, S. F. Improving Performance in Colloidal Quantum Dot Solar Cells by Tuning Band Alignment through Surface Dipole Moments. *J. Phys. Chem. C* **2015**, *119*, 2996-3005.
217. Yang, S., Prendergast, D., Neaton, J. B. Tuning Semiconductor Band Edge Energies for Solar Photocatalysis via Surface Ligand Passivation. *Nano Lett.* **2012**, *12*, 383-388.
218. Carroll, G. M., Brozek, C. K., Hartstein, K. H., Tsui, E. Y., Gamelin, D. R. Potentiometric Measurements of Semiconductor Nanocrystal Redox Potentials. *J. Am. Chem. Soc.* **2016**, *138*, 4310-4313.
219. Carroll, G. M., Tsui, E. Y., Brozek, C. K., Gamelin, D. R. Spectroelectrochemical Measurement of Surface Electrostatic Contributions to Colloidal CdSe Nanocrystal Redox Potentials. *Chem. Mater.* **2016**, *28*, 7912-7918.
220. Hu, K., Brust, M., Bard, A. J. Characterization and Surface Charge Measurement of Self-Assembled CdS Nanoparticle Films. *Chem. Mater.* **1998**, *10*, 1160-1165.
221. Schival, K. A., Gipson, R. R., Prather, K. V., Tsui, E. Y. Photoinduced Surface Charging in Iron-Carbonyl-Functionalized Colloidal Semiconductor Nanocrystals. *Nano Lett.* **2019**, *19*, 7770-7774.
222. Prather, K. V., Lee, S., Tsui, E. Y. Metal-Carbonyl-Functionalized CdSe Nanocrystals: Synthesis, Surface Redox, and Infrared Intensities. *Inorg. Chem.* **2021**, *60*, 4269-4277.
223. Prather, K. V., Stoffel, J. T., Tsui, E. Y. Z-Type Ligand Coordination at Colloidal Semiconductor Nanocrystals Modifies Surface Electrostatics. *Chem. Mater.* **2022**, *34*, 3976-3984.
224. Ertl, G., Neumann, M., Streit, K. M. Chemisorption of CO on the Pt(111) surface. *Surf. Sci.* **1977**, *64*, 393-410.

225. Carrasco, E., Aumer, A., Brown, M. A., Dowler, R., Palacio, I., Song, S., Sterrer, M. Infrared spectra of high coverage CO adsorption structures on Pt(111). *Surf. Sci.* **2010**, *604*, 1320-1325.
226. Greenler, R. G., Snider, D. R., Witt, D., Sorbello, R. S. The metal-surface selection rule for infrared spectra of molecules adsorbed on small metal particles. *Surf. Sci.* **1982**, *118*, 415-428.
227. Fried, S. D., Boxer, S. G. Measuring Electric Fields and Noncovalent Interactions Using the Vibrational Stark Effect. *Acc. Chem. Res.* **2015**, *48*, 998-1006.
228. Goldman, A. S., Krogh-Jespersen, K. Why Do Cationic Carbon Monoxide Complexes Have High C−O Stretching Force Constants and Short C−O Bonds? Electrostatic Effects, Not σ-Bonding. *J. Am. Chem. Soc.* **1996**, *118*, 12159-12166.
229. Saniepay, M., Mi, C., Liu, Z., Abel, E. P., Beaulac, R. Insights into the Structural Complexity of Colloidal CdSe Nanocrystal Surfaces: Correlating the Efficiency of Nonradiative Excited-State Processes to Specific Defects. *J. Am. Chem. Soc.* **2018**, *140*, 1725-1736.
230. Zhang, Z., Edme, K., Lian, S., Weiss, E. A. Enhancing the Rate of Quantum-Dot-Photocatalyzed Carbon–Carbon Coupling by Tuning the Composition of the Dot's Ligand Shell. *J. Am. Chem. Soc.* **2017**, *139*, 4246-4249.
231. Caputo, J. A., Frenette, L. C., Zhao, N., Sowers, K. L., Krauss, T. D., Weix, D. J. General and Efficient C–C Bond Forming Photoredox Catalysis with Semiconductor Quantum Dots. *J. Am. Chem. Soc.* **2017**, *139*, 4250-4253.
232. Widness, J. K., Enny, D. G., McFarlane-Connelly, K. S., Miedenbauer, M. T., Krauss, T. D., Weix, D. J. CdS Quantum Dots as Potent Photoreductants for Organic Chemistry Enabled by Auger Processes. *J. Am. Chem. Soc.* **2022**, *144*, 12229-12246.
233. Jiang, Y., Weiss, E. A. Colloidal Quantum Dots as Photocatalysts for Triplet Excited State Reactions of Organic Molecules. *J. Am. Chem. Soc.* **2020**, *142*, 15219-15229.
234. Qiao, J., Song, Z.-Q., Huang, C., Ci, R.-N., Liu, Z., Chen, B., Tung, C.-H., Wu, L.-Z. Direct, Site-Selective and Redox-Neutral α-C−H Bond Functionalization of Tetrahydrofurans via Quantum Dots Photocatalysis. *Angew. Chem. Int. Ed.* **2021**, *60*, 27201-27205.
235. Weiss, E. A. Designing the Surfaces of Semiconductor Quantum Dots for Colloidal Photocatalysis. *ACS Energy Lett.* **2017**, *2*, 1005-1013.
236. Kodaimati, M. S., McClelland, K. P., He, C., Lian, S., Jiang, Y., Zhang, Z., Weiss, E. A. Viewpoint: Challenges in Colloidal Photocatalysis and Some Strategies for Addressing Them. *Inorg. Chem.* **2018**, *57*, 3659-3670.
237. Huang, Z., Tang, M. L. Designing Transmitter Ligands That Mediate Energy Transfer between Semiconductor Nanocrystals and Molecules. *J. Am. Chem. Soc.* **2017**, *139*, 9412-9418.
238. Peterson, M. D., Jensen, S. C., Weinberg, D. J., Weiss, E. A. Mechanisms for Adsorption of Methyl Viologen on CdS Quantum Dots. *ACS Nano* **2014**, *8*, 2826-2837.
239. Prier, C. K., Rankic, D. A., MacMillan, D. W. C. Visible Light Photoredox Catalysis with Transition Metal Complexes: Applications in Organic Synthesis. *Chem. Rev.* **2013**, *113*, 5322-5363.

For Table of Contents Only